

# Outer Dowsing Offshore Wind

## Environmental Statement

Chapter 7 Marine Physical  
Processes

Volume 3 Appendices

Appendix 7.2

Date: March 2024

Pursuant to APFP Regulation: 5(2)(a)

Document Reference: 6.3.7.2



Company:	<b>Outer Dowsing Offshore Wind</b>	Asset:	<b>Whole Asset</b>			
Project:	<b>Whole Wind Farm</b>	Sub Project/Package:	Whole Asset			
Document Title or Description:	Chapter 7 Marine Physical Processes					
Internal Document Number:	PP1-ODOW-DEV-CS-REP-0162	3 <sup>rd</sup> Party Doc No (If applicable):	N/A			
<i>Outer Dowsing Offshore Wind accepts no liability for the accuracy or completeness of the information in this document nor for any loss or damage arising from the use of such information.</i>						
Rev No.	Date	Status / Reason for Issue	Author	Checked by	Reviewed by	Approved by
V1.0	March 2024	Final	GoBe	GoBe	Shepherd and Wedderburn	ODOW



# MetOceanWorks

## Outer Dowsing Offshore Wind. Annex C: EIA - Marine Physical Processes Numerical Modelling

21 February 2024

MetOceanWorks Reference:

GoBe\_C00003\_R04\_Marine\_Physical\_Processes\_Modelling

Commercial in Confidence

Andrew Watson MSc CSci CMarSci MIMarEST

Senior Metocean Consultant & Director

[andrew.watson@metoceanworks.com](mailto:andrew.watson@metoceanworks.com)

Contact +44 (0)7763 896635

MetOceanWorks Ltd is Registered in England and Wales, Company Number 8078702

Revision	Description	Prepared	Reviewed	Date
R05	EIA – Changed ECC Boundaries	Jamie Hernon	Bill Cooper	21 February 2024
R04	EIA - Final	Jamie Hernon	Bill Cooper	23 January 2024
R03	EIA - Draft	Jamie Hernon	Bill Cooper	22 September 2023
R02	PEIR - Final	Jamie Hernon	Julia Bolton, Claire Hinton and Bill Cooper	7 February 2023
R01	PEIR – Draft	Jamie Hernon	Bill Cooper	1 February 2023



## Disclaimer

MetOceanWorks has prepared this report for the sole use of the client and for the intended purposes as stated in the agreement between MetOceanWorks and the client under which this report was completed. MetOceanWorks has exercised due and customary care in preparing this report but has not, save as specifically stated, independently verified information provided by others. No other warranty, express or implied, is made in relation to the contents of this report. The use of this report, or reliance on its content, by unauthorised third parties without written permission from MetOceanWorks shall be at their own risk, and MetOceanWorks accepts no duty of care to such third parties. Any recommendations, opinions or findings stated in this report are based on facts and circumstances as they existed at the time the report was prepared. Any changes in such facts and circumstances may adversely affect the recommendations, opinions or findings contained in this report.



## Table of contents

<b>1</b>	<b>Definitions.....</b>	<b>1</b>
1.1	Units and Conventions .....	1
1.2	Glossary of commonly used terms.....	1
<b>2</b>	<b>Introduction .....</b>	<b>2</b>
2.1	Background.....	2
2.2	Report Structure .....	3
<b>3</b>	<b>Common Modelling Inputs.....</b>	<b>4</b>
3.1	Bathymetry.....	4
3.2	Coastline.....	6
3.3	Wind.....	6
<b>4</b>	<b>Hydrodynamics .....</b>	<b>7</b>
4.1	Measured Hydrodynamic Data .....	7
4.2	Modelling Software.....	8
4.3	Model Boundary Conditions and Spatial Extent .....	8
4.4	Model Validation.....	10
4.5	Selection of Tidal Events.....	23
4.6	Hydrodynamic Blockage Modelling.....	23
<b>5</b>	<b>Waves .....</b>	<b>24</b>
5.1	Measured Wave Data.....	24
5.2	Modelling Software.....	25
5.3	Model Boundary Conditions .....	26
5.4	Model Validation.....	27
5.5	Selection of Wave Events .....	31
5.6	Wave Blockage Modelling .....	31
<b>6</b>	<b>Particle Tracking.....</b>	<b>32</b>
6.1	Array Area.....	33
6.1.1	Inter Array Cabling – Mass Flow Excavator Trenching.....	33
6.1.2	Inter Array Cabling – Sandwave Clearance .....	34
6.1.3	Foundation Installation – Drilling .....	34
6.1.4	Foundation Installation – Bed Levelling.....	34



## Marine Physical Processes – Numerical Modelling

---

6.2	Export Cable Route.....	34
6.2.1	HDD Punch-out - Bentonite Release.....	34
6.2.2	Sandwave Clearance.....	35
6.2.3	Mass Flow Excavator Trenching .....	35
<b>7</b>	<b>Results.....</b>	<b>36</b>
	<b>References.....</b>	<b>37</b>



## List of Figures

Figure 2.1: Overview of the Project including the windfarm and ECC .....	2
Figure 3.1: Coverage of OceanWise data, and DTM tiles procured shown in green. ....	4
Figure 3.2: Coverage of the Project’s supplied site-specific survey bathymetry.....	5
Figure 4.1: Measured datasets considered for hydrodynamic model validation. ....	8
Figure 4.2 European MIKE21 flexible model mesh. Bathymetry in m MSL .....	9
Figure 4.3: Comparison of measured and modelled water levels at Whitby. ....	11
Figure 4.4: Comparison of measured and modelled water levels at Cromer.....	11
Figure 4.5: Comparison of measured and modelled water levels at the Project Seabed Frame. ....	12
Figure 4.6: Comparison of measured and modelled depth-average currents, the Project Seabed Frame.....	13
Figure 4.7: Comparison of measured and modelled depth-average currents, the Project FLS.....	13
Figure 4.8: Comparison of measured and modelled depth-average currents, M7 Seabed Frame.....	14
Figure 4.9: Comparison of measured and modelled depth-average currents, Race Bank.....	14
Figure 4.10: Time-series comparison of modelled and measured depth-average current speeds, the Project Seabed Frame. ....	15
Figure 4.11: Time-series comparison of modelled and measured depth-average current directions, the Project Seabed Frame. ....	16
Figure 4.12: Time-series comparison of modelled and measured depth-average current speeds, the Project FLS. ....	17
Figure 4.13: Time-series comparison of modelled and measured depth-average current directions, the Project FLS. ....	18
Figure 4.14: Time-series comparison of modelled and measured depth-average current speeds, M07 Seabed Frame.....	19
Figure 4.15: Time-series comparison of modelled and measured depth-average current directions, M07 Seabed Frame.....	20
Figure 4.16: Time-series comparison of modelled and measured depth-average current speeds, Race Bank....	21
Figure 4.17: Time-series comparison of modelled and measured depth-average current directions, Race Bank. ....	22
Figure 5.1: Locations of the wave measurement devices. ....	25
Figure 5.2: Wave model domains.....	26
Figure 5.3. Outer Dowsing, Hm0 validation, all data. ....	28
Figure 5.4. Outer Dowsing, Tp validation, all data.....	28
Figure 5.5. Outer Dowsing, Tm02 validation, all data.....	29
Figure 5.6. Chapel Point, Hm0 validation, all data.....	29
Figure 5.7. Chapel Point, Tp validation, all data. ....	30
Figure 5.8. Chapel Point, Tm02 validation, all data. ....	30
Figure 6.1. Locations used in particle tracking modelling.....	33



---

## List of Tables

Table 4.1: Measured datasets considered for hydrodynamic model validation. ....	7
Table 4.2: Events selected for hydrodynamic modelling. ....	23
Table 5.1: Measured datasets used for wave model validation. ....	24
Table 5.2: Wave model domains. ....	26
Table 5.3: Wave conditions modelled. ....	31
Table 6.1: Details of the representative sediment types. ....	32





# 1 Definitions

## 1.1 Units and Conventions

The following list describes the units and conventions used in this report. Units have been expressed using the International System of Units (SI) convention, with the exception that, at the request of GoBe, spaces before unit symbols are not used.

- Wave direction is expressed in compass points or degrees, relative to true North [°T], and describes the direction **from** which the waves are propagating.
- Wave heights are expressed in metres [m].
- Wave periods are expressed in seconds [s].
- Current direction is expressed in compass points or degrees, relative to true North [°T], and describes the direction **towards** which the currents are flowing.
- Current speeds are expressed in metres per second [m/s].
- Water levels are expressed in metres [m].
- Positions are quoted relative to WGS 84 except where stated.
- All times are quoted in Coordinated Universal Time [UTC].

## 1.2 Glossary of commonly used terms

The following list describes common metocean terms used throughout this report.

Waves	Description
Hm0	Significant wave height. Approximately the average height of the highest one third of the waves in a defined period, estimated from the wave spectrum as $4\sqrt{m_0}$ .
$m_0, m_1, m_2$	The zeroth, first and second moments of the wave spectrum respectively.
$T_p$	The spectral peak wave period. The wave period at which most energy is present in the wave spectrum.
$T_{m02}$	The mean zero-crossing wave period. Estimated from the wave spectrum as $\sqrt{m_0/m_2}$ .
Currents	Description
Current speed	Magnitude of local current flow.
Offshore Construction	Description
TSHD	Trailing suction hopper dredger. Self-propelled vessel able to vacuum sediments from the seafloor to a hopper in the hull, for subsequent discharge elsewhere.
ECC	Offshore Export Cable Corridor.
WTG	Wind Turbine Generator.
OSS	Offshore Sub-Station.
ANS	Artificial Nesting Structure.
ORCP	Offshore Reactive Compensation Platform.
HDD	Horizontal Directional Drilling. Method of installing underground cables using a drill.



## 2 Introduction

### 2.1 Background

GoBe Consultants Ltd contracted MetOceanWorks (working in partnership with Cooper Marine Advisors) to provide support in the delivery of the marine processes environmental impact assessment (EIA) chapter, and to provide relevant marine processes modelling services for Outer Dowsing Offshore Wind (hereafter referred to as 'the Project').

The Project is located approximately 50km off the Lincolnshire coast in water depths of approximately 9 to 50m. A subsea cable will link the windfarm with the power delivery network at the adjacent coast. Figure 2.1 shows the proposed windfarm lease zone and the proposed export cable corridor (ECC). Numerical modelling has been carried out to assess the likely impact of the construction and operation of the windfarm and its associated infrastructure, on the marine environment.

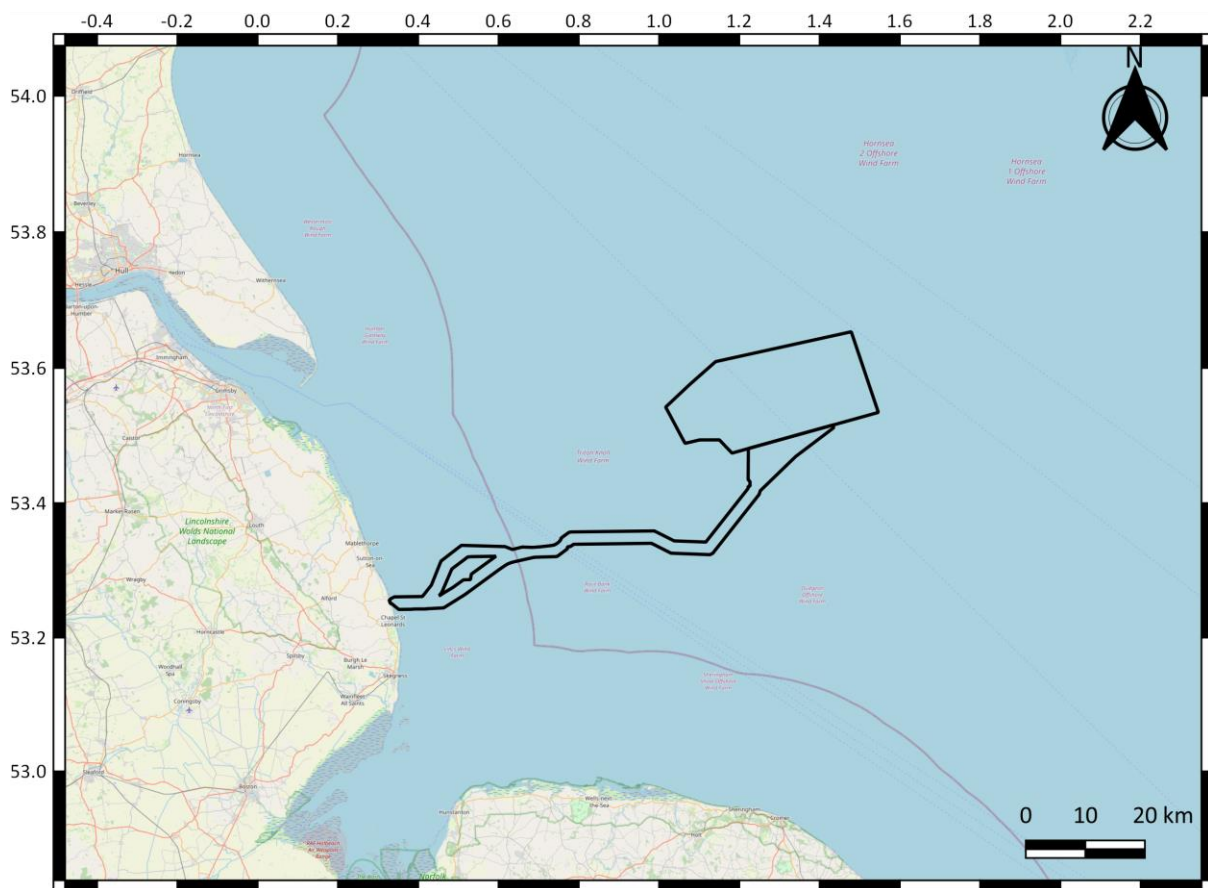


Figure 2.1: Overview of the Project including the windfarm and ECC.



## 2.2 Report Structure

This document describes the various data sources, marine process models and analysis methods used throughout the study. This document is a companion document to Annex A [1] and B [2].

Modelling details are discussed in Sections 3 to 6, initially introducing common model inputs (Section 3) before moving onto the models themselves. By way of introduction to the overall approach:

- **Hydrodynamics** were modelled using the MIKE21FM 2D flexible mesh modelling package. Modelled currents and water levels have been validated against measurements from several locations. See Section 4 for details. The validated hydrodynamic model was then used to simulate blockages to flows caused by the presence of the built structures, and to drive the particle tracking module.
- The **Particle Tracking** module was used to simulate the extent and fate of sediments disturbed during construction activities (Section 6).
- **Waves** were modelled with a bespoke SWAN (Simulating Waves Nearshore) model with high resolution regional nests. The model has been extensively validated against measured datasets in the region. See Section 5 for details. The model was then used to simulate blockages to waves caused by the presence of the built structures.

Thereafter, Section 7 provides a description of the results. The document concludes with a list of the references used throughout.



## 3 Common Modelling Inputs

### 3.1 Bathymetry

A representative bathymetry dataset was required as input to the wave and hydrodynamic models. This was achieved by merging three different datasets which originated from:

- European Marine Observation and Data Network (EMODnet) (regional composite);
- OceanWise (regional composite); and
- The Project's survey data for the development area.

Far-field bathymetry data for the models were sourced from the EMODnet Bathymetry Data Portal [3]. EMODnet provides a service for viewing and downloading a harmonised Digital Terrain Model (DTM) for the European sea regions that is generated by an ever-increasing number of bathymetric survey data sets provided by national hydrographic institutions, research bodies and academia. As of 2018, these data are available at a grid resolution of approximately 130m.

These data were then augmented with OceanWise raster charts supplied by MarineFIND and which have a resolution of 1 arc-second (or approximately 25m, depending on latitude), whereby physical features such as trenches, ridges, sand banks and sand waves are well represented. Figure 3.1 shows the available coverage of OceanWise data with the tiles procured highlighted in green.

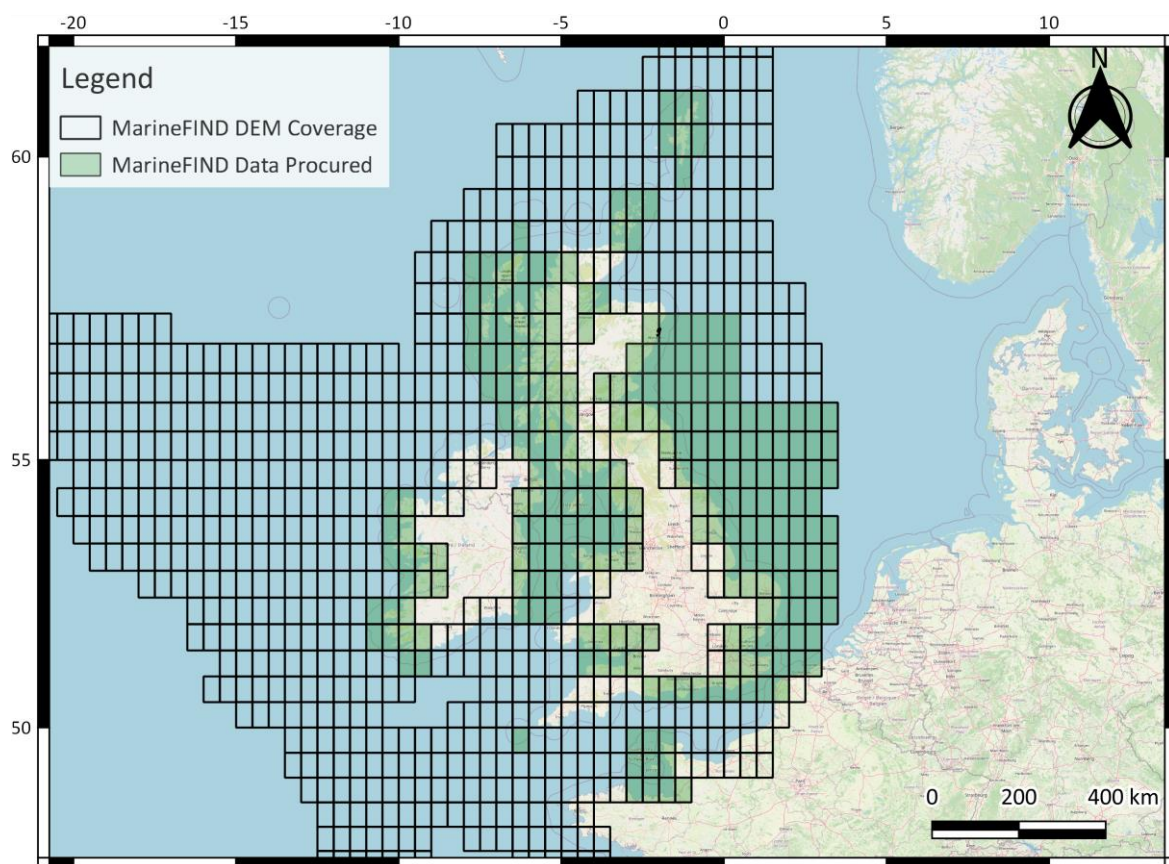


Figure 3.1: Coverage of OceanWise data, and DTM tiles procured shown in green.



These data were merged with bathymetry supplied by the Project to MetOceanWorks under a separate contract [4]. Data from two survey campaigns were provided, covering the array area and the ECC, respectively. The total coverage of both surveys is shown in Figure 3.2.

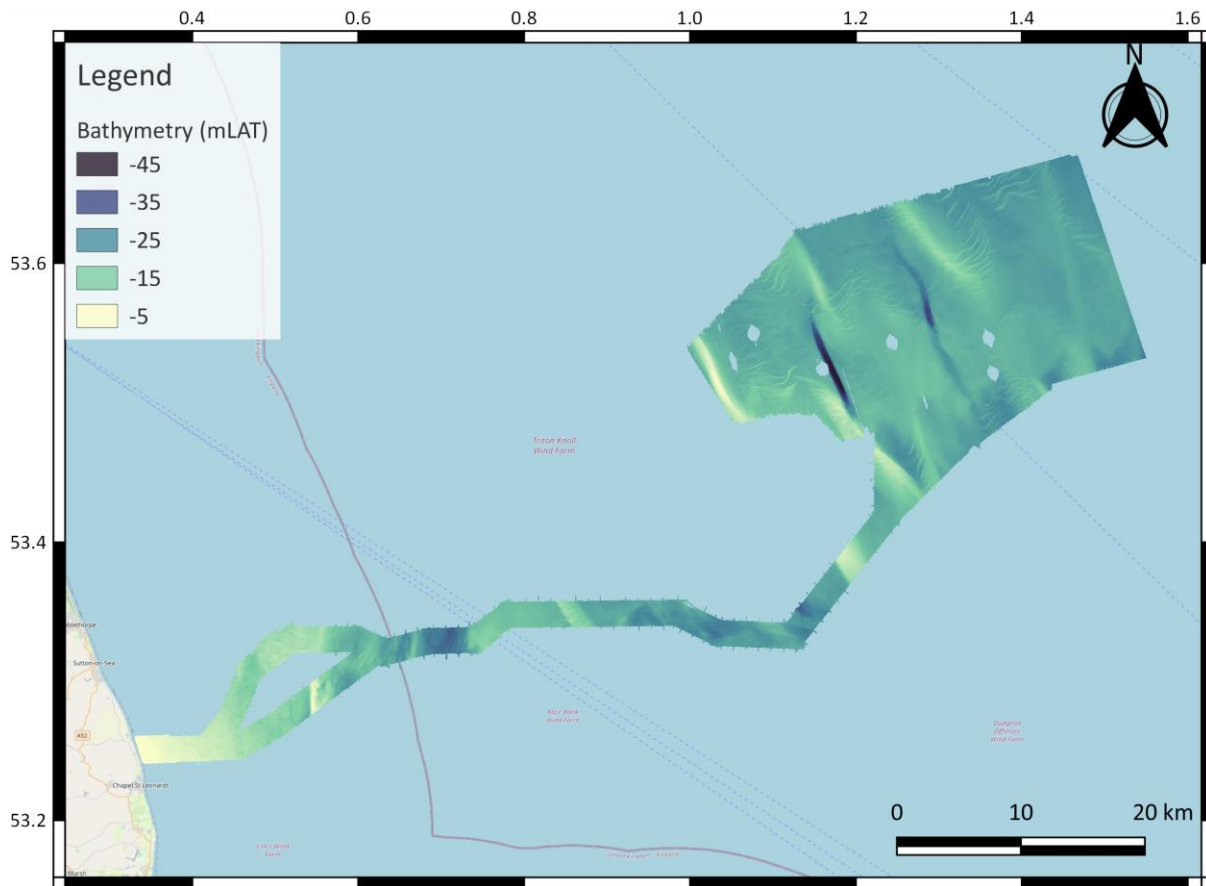


Figure 3.2: Coverage of the Project's supplied site-specific survey bathymetry.

A quality check of the vertical consistency of the two project surveys revealed that there were discrepancies in the overlapping portions of the datasets. Comparison against the OceanWise data and the presence of several sharp vertical gradients in the array area survey dataset suggested that the ECC survey was likely to be the most reliable dataset in terms of vertical datum. Therefore, the array area survey was adjusted such that the mean height of the areas overlapping with the ECC survey was the same as that for those areas of the ECC survey. The various holes in the array area survey around oil and gas infrastructure and data buoys were filled using an interpolation routine.

A critical aspect of the bathymetry development for the numerical modelling purposes was to ensure no vertical discontinuities at the boundaries between the OceanWise and site-specific survey data. Therefore, the two datasets were merged using a cosine tapering method to avoid sudden vertical shifts at dataset edges.

The bathymetry data were converted from LAT to MSL datum prior to use, as required by both the SWAN and MIKE21 modelling software. These datum differences were calculated from the Finite Element Solution FES2014 dataset, a 35-constituent, global tidal database available from AVISO [5].





### 3.2 Coastline

The coastline of England was discretised into the models using the Boundary-Line™ mean high water mark vector product, from the Ordnance Survey, which describes the position of Mean High Water Springs. These data were used in conjunction with satellite imagery to provide the most accurate and appropriate coastline description for the models.

### 3.3 Wind

European Centre for Medium-Range Weather Forecasts (ECMWF) ReAnalysis 5 (ERA5) wind data was used to drive the hydrodynamic and wave models. ERA5 is the fifth and latest major global reanalysis produced by ECMWF. Hourly wind speeds are available for the period 1979 to near-present at various atmospheric levels (including at 10m above sea level, as used to drive the wave and hydrodynamic models) are available on a 0.25° by 0.25° resolution grid via the Copernicus Climate Change Service (C3S) Climate Data Store (CDS). Prior to use, the raw ERA5 data was calibrated using a bespoke adjustment developed by MetOceanWorks which improves performance in driving models.



## 4 Hydrodynamics

Current and water level parameters were produced using a European, basin-scale flexible mesh hydrodynamic model. Depth-averaged currents and water levels were produced to drive the particle tracking model (described in Section 6), and to predict the blocking effect of the built structures.

Prior to use in the assessments, the performance of the model in representing currents and water levels was ascertained by comparison against several measured data sources. These are described in Section 4.1.

### 4.1 Measured Hydrodynamic Data

To support calibration and validation of the hydrodynamic model, measured data were acquired from the British Oceanographic Data Centre (BODC), UK National Tide Gauge Network and the Marine Data Exchange, as well as those provided by the Project. An overview of the measured datasets can be found in Table 4.1 and Figure 4.1.

Table 4.1: Measured datasets considered for hydrodynamic model validation.

Dataset	Parameter	Supplier	Location	Time Period	* Water Depth [mLAT]
<b>Cromer</b>	Water Levels	BODC	52.9344°N, 1.3016°E	1-Jan-1988 to near-present	Coastal
<b>Whitby</b>	Water Levels	BODC	54.4900°N, 0.6100°W	1-Jan-1980 to near-present	Coastal
<b>Floating LiDAR System (FLS)</b>	Water Levels (erroneous) and Currents	The Project	53.5872°N, 1.2826°E	17-Apr-2022 to 17-Aug-2022	23.3
<b>Seabed Frame</b>	Water Levels and Currents	The Project	53.6244°N, 1.4150°E	17-Apr-2022 to 04-Aug-2022	21.8
<b>Race Bank</b>	Currents	Marine Data Exchange	53.3119°N, 0.7487°E	24-Jun-2006 to 21-Aug-2006	7.6
<b>M7 Seabed Frame</b>	Currents	Marine Data Exchange	53.7677°N, 0.1942°E	1-Mar-2022 to 24-May-2022	17.9

\* The term "Coastal" is used to denote an instrument mounted to a harbour wall or pier.

The measurements were carefully reviewed prior to use and in general required no additional quality control beyond that which was undertaken by the originator, however the water level measurements from the FLS are clearly erroneous and were therefore rejected. Current profiles were reduced to equivalent depth-average values by averaging the horizontal velocity components that occurred between 30% and 50% of the height above bed. This is consistent with the theoretical power law whereby depth-average currents occur at approximately 40% of the height above bed. With regards to water level data quality, the highest confidence can be placed in measurements from the coastal tide gauges although it should be noted that, although short in duration, the site-specific measurements from the Project's Seabed Frame (Seaguard) are of a high standard. With respect to current observations, the highest confidence can be placed in the most recent measurements from the Seabed Frame and FLS mounted current profiler. However, the earlier Race Bank measurements, whilst relatively short, are also of good quality.

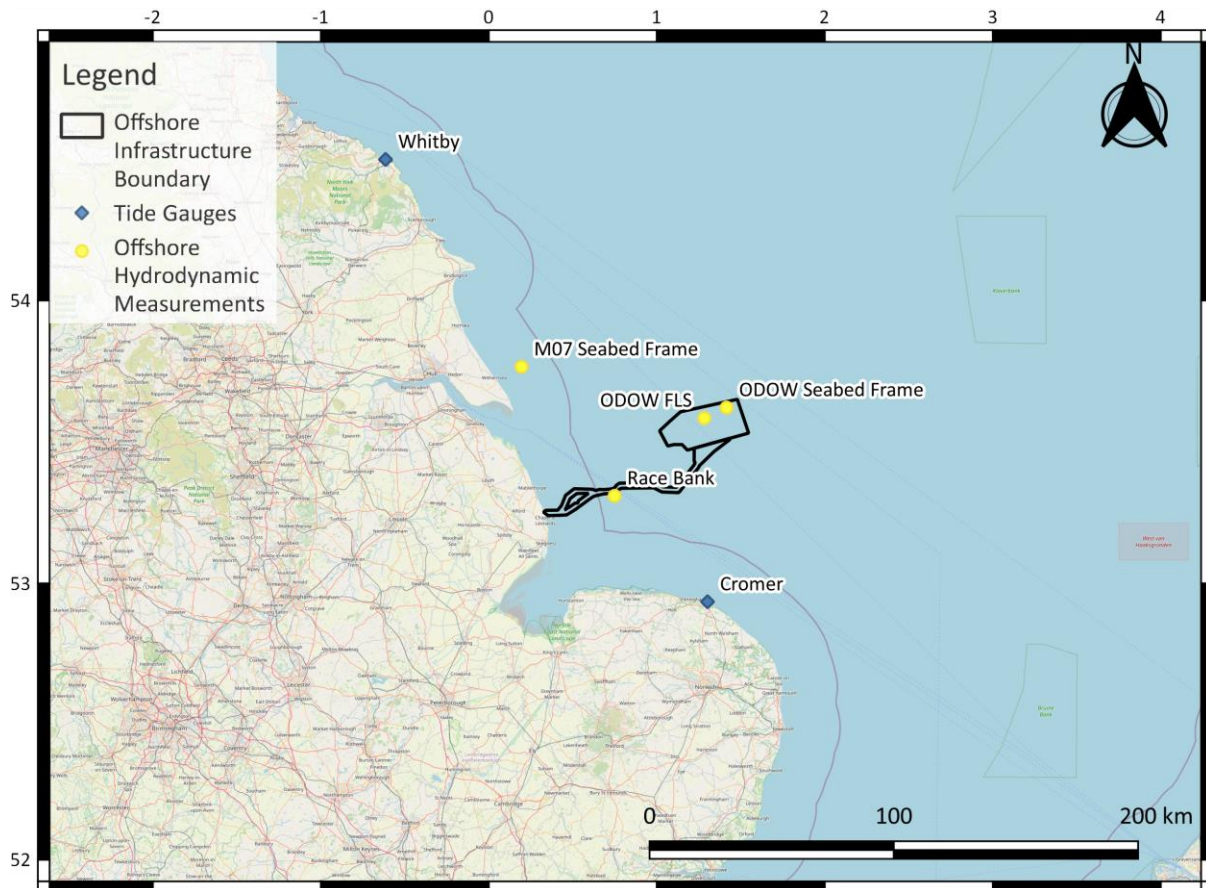


Figure 4.1: Measured datasets considered for hydrodynamic model validation.

## 4.2 Modelling Software

The hydrodynamic model has been developed using the MIKE21FM (Flexible Mesh) 2D modelling package [6] [7], a comprehensive modelling system for two-dimensional water modelling developed by DHI.

## 4.3 Model Boundary Conditions and Spatial Extent

Tidal boundary conditions to the European model originate from the Finite Element Solution FES2014 dataset. This 35 tidal constituent global data-set has been produced using numerical modelling which assimilates satellite observations of water level and has, in our opinion, the best skill of any publicly-available global tide model. The dataset includes tide elevations (amplitude and phase) and tide currents on a  $0.0625^\circ$  grid (approximately 7.0km in latitude and 3.8km in longitude in the region of interest). The model was driven using water levels varying along three open boundaries, as shown in the top left panel of Figure 4.2.



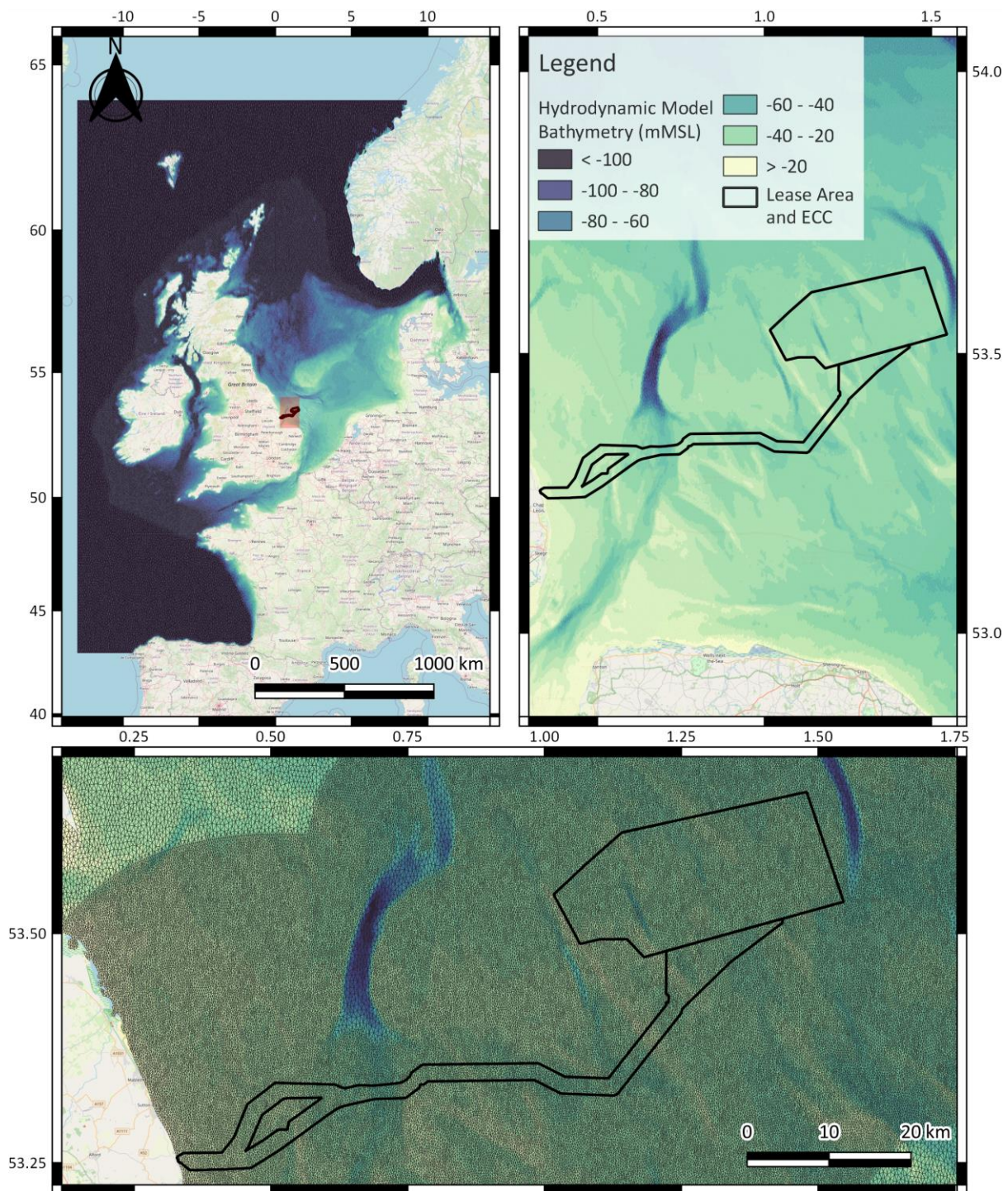


Figure 4.2 European MIKE21 flexible model mesh. Bathymetry in m MSL.

The model had a spatial resolution of 200m within a 30km buffer of the array area and ECC, with the exception of deep channels such as the Inner Silver Pit, or the Sole Pit, which were discretised at a spatial resolution of 400m. Outside of this area to 55km from the development, a resolution of 400m was used, and then a resolution of 800m was used to 100km from the development. A 3km resolution is used in the remainder of the Southern North Sea.



Atmospheric forcing for the hydrodynamic model originated from the ECMWF ERA5 dataset and was applied to ensure that atmospheric driven surge effects were properly represented in the model. This comprised of MetOceanWorks-adjusted wind speeds, unadjusted wind directions, and unadjusted pressure fields.

#### 4.4 Model Validation

Predicted water levels are compared against water level measurements in Figure 4.3 to Figure 4.5 to demonstrate model performance. With low mean error, a correlation coefficient close to unity and a low scatter index, this comparison demonstrates excellent model skill.

Current speed validation plots and time series plots are presented in Figure 4.6 to Figure 4.17. These statistical and time series comparisons of modelled and measured depth-averaged current speeds and directions demonstrate good overall performance, in particular with flood and ebb asymmetry being well reproduced by the model.





From	01-Jan-2013
To	31-Dec-2013
Mean (X)	-0.00
Mean (Y)	-0.01
N	31225
Bias	-0.01
AME	0.10
RMS	0.13
SI	0.05
CC	1.00
R <sup>2</sup>	0.99

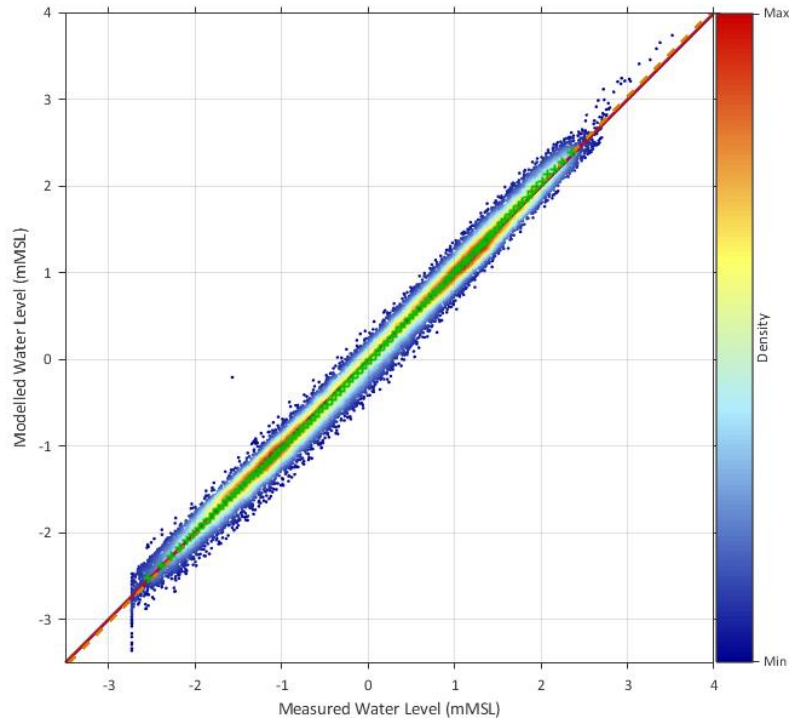


Figure 4.3: Comparison of measured and modelled water levels at Whitby.

From	05-Jan-2013
To	31-Dec-2013
Mean (X)	-0.07
Mean (Y)	-0.06
N	28010
Bias	0.01
AME	0.14
RMS	0.18
SI	0.05
CC	0.99
R <sup>2</sup>	0.98

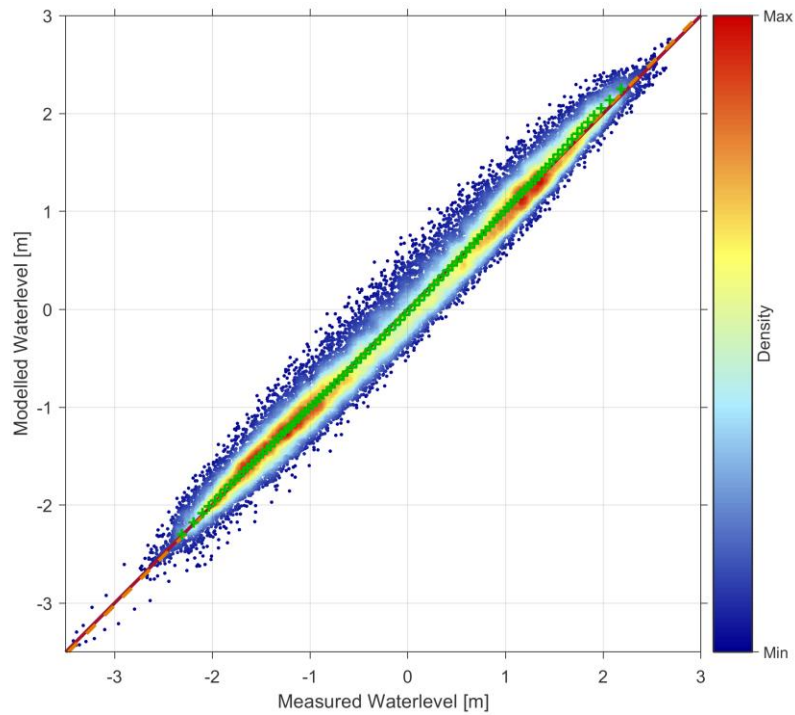
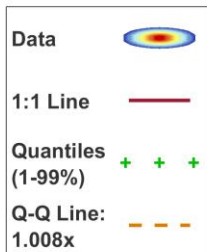


Figure 4.4: Comparison of measured and modelled water levels at Cromer.



<b>From</b>	17-Apr-2022
<b>To</b>	04-Aug-2022
<b>Mean (X)</b>	-0.00
<b>Mean (Y)</b>	0.01
<b>N</b>	15670
<b>Bias</b>	0.01
<b>AME</b>	0.13
<b>RMS</b>	0.16
<b>SI</b>	0.07
<b>CC</b>	0.99
<b>R<sup>2</sup></b>	0.97

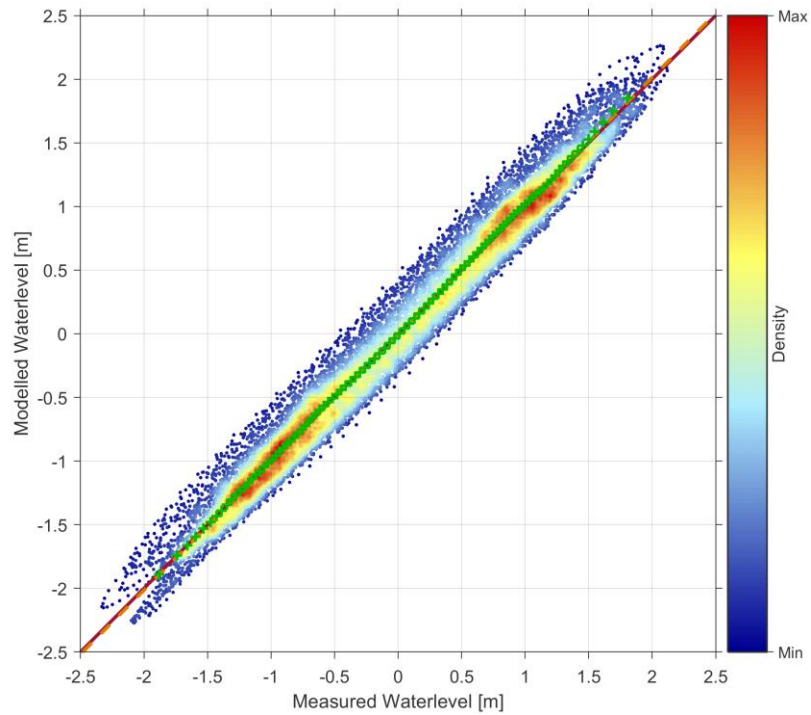
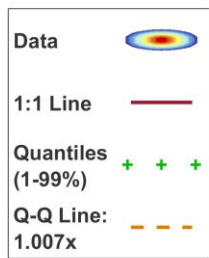


Figure 4.5: Comparison of measured and modelled water levels at the Project Seabed Frame.



From	17-Apr-2022
To	04-Aug-2022
Mean (X)	0.44
Mean (Y)	0.44
N	78351
Bias	0.00
AME	0.05
RMS	0.07
SI	0.15
CC	0.96
R <sup>2</sup>	0.92

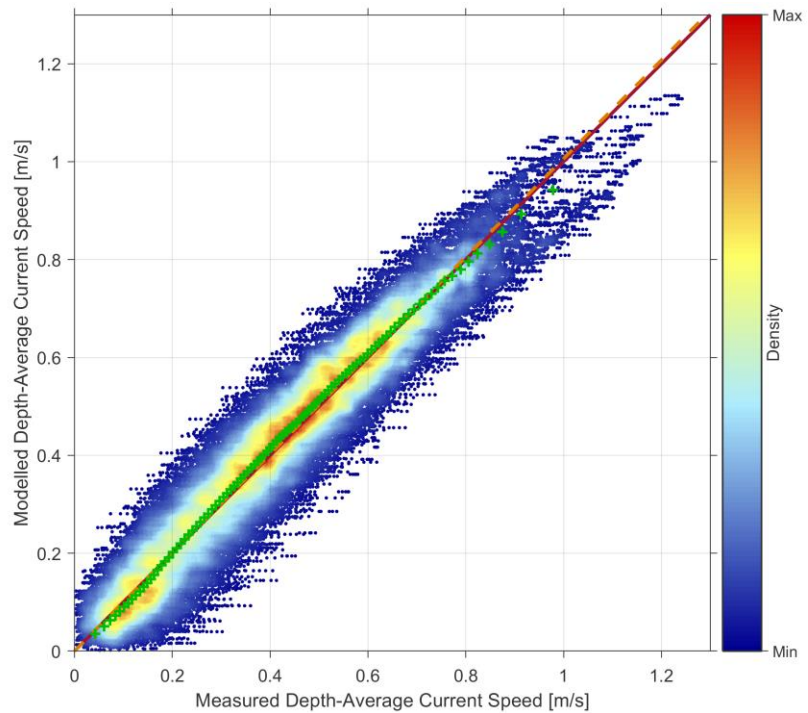
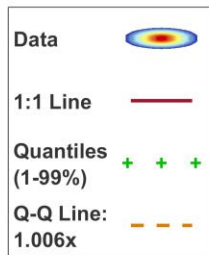


Figure 4.6: Comparison of measured and modelled depth-average currents, the Project Seabed Frame.

From	17-Apr-2022
To	17-Aug-2022
Mean (X)	0.46
Mean (Y)	0.47
N	17554
Bias	0.02
AME	0.06
RMS	0.08
SI	0.17
CC	0.95
R <sup>2</sup>	0.90

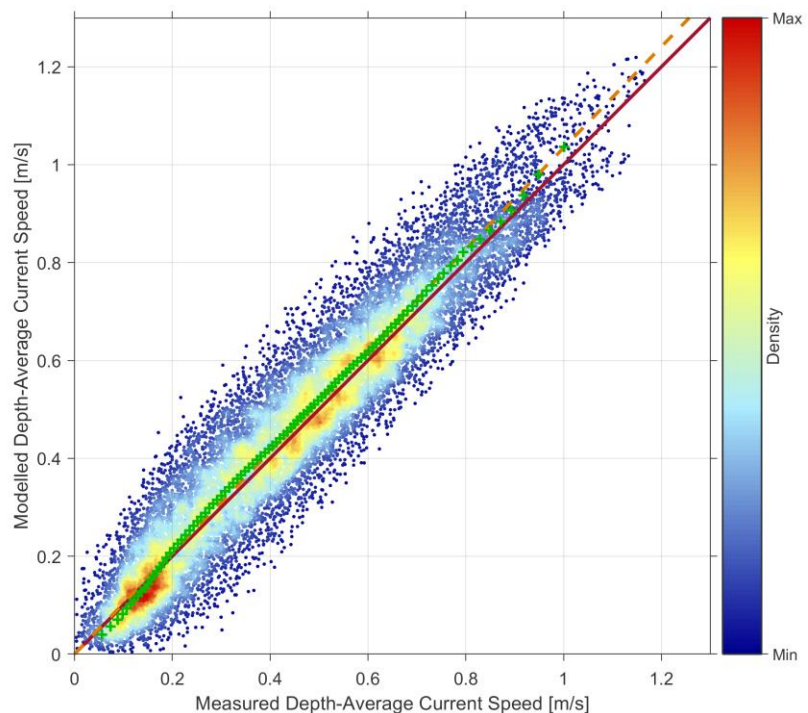
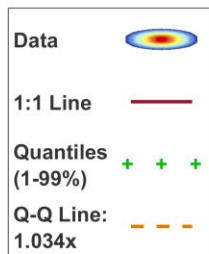


Figure 4.7: Comparison of measured and modelled depth-average currents, the Project FLS.



From	05-Mar-2022
To	24-May-2022
Mean (X)	0.46
Mean (Y)	0.46
N	11456
Bias	0.01
AME	0.05
RMS	0.06
SI	0.13
CC	0.97
R <sup>2</sup>	0.94

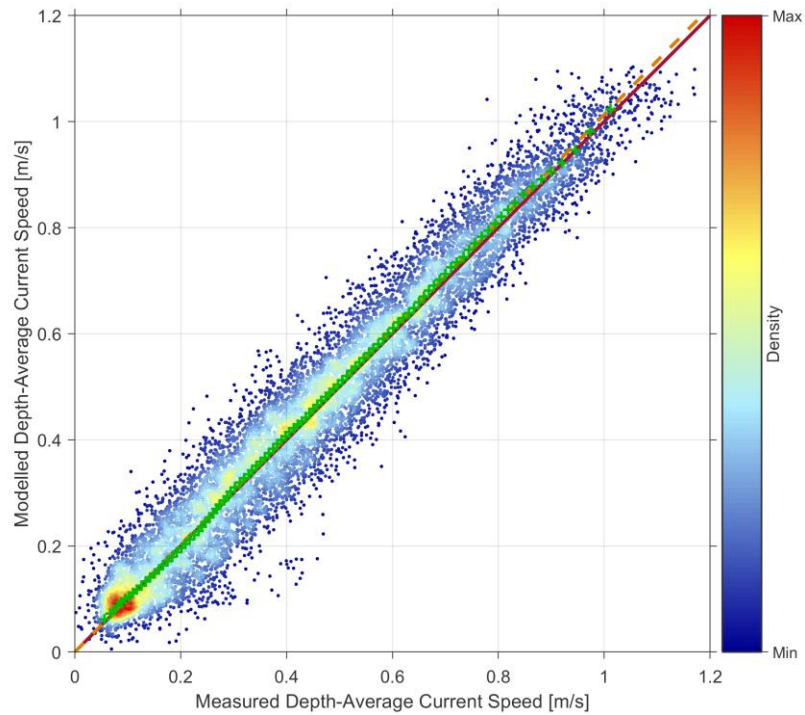
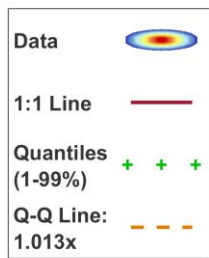


Figure 4.8: Comparison of measured and modelled depth-average currents, M7 Seabed Frame.

From	24-Jun-2006
To	21-Aug-2006
Mean (X)	0.56
Mean (Y)	0.60
N	8307
Bias	0.04
AME	0.07
RMS	0.09
SI	0.14
CC	0.91
R <sup>2</sup>	0.84

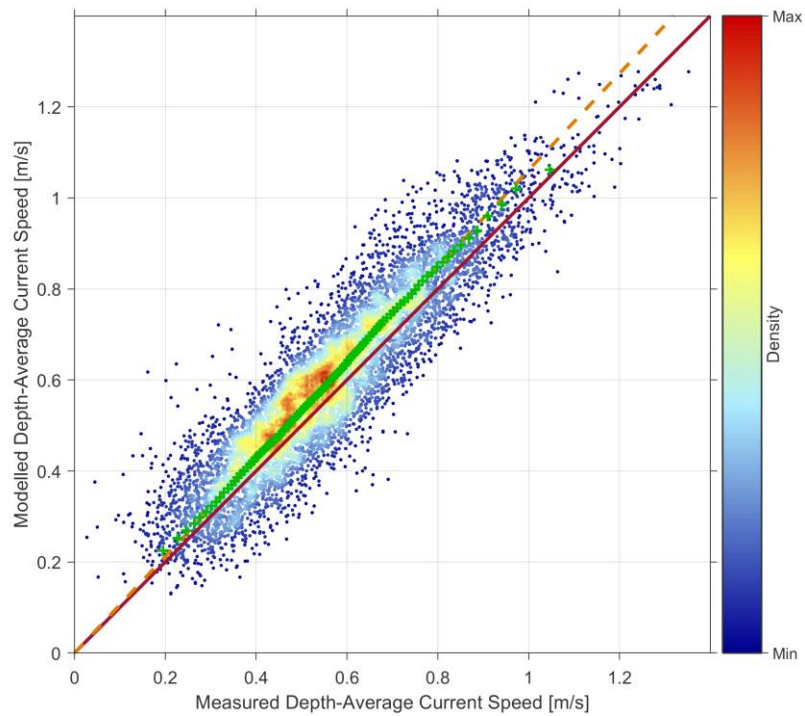
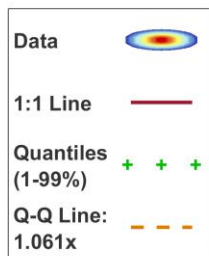


Figure 4.9: Comparison of measured and modelled depth-average currents, Race Bank.

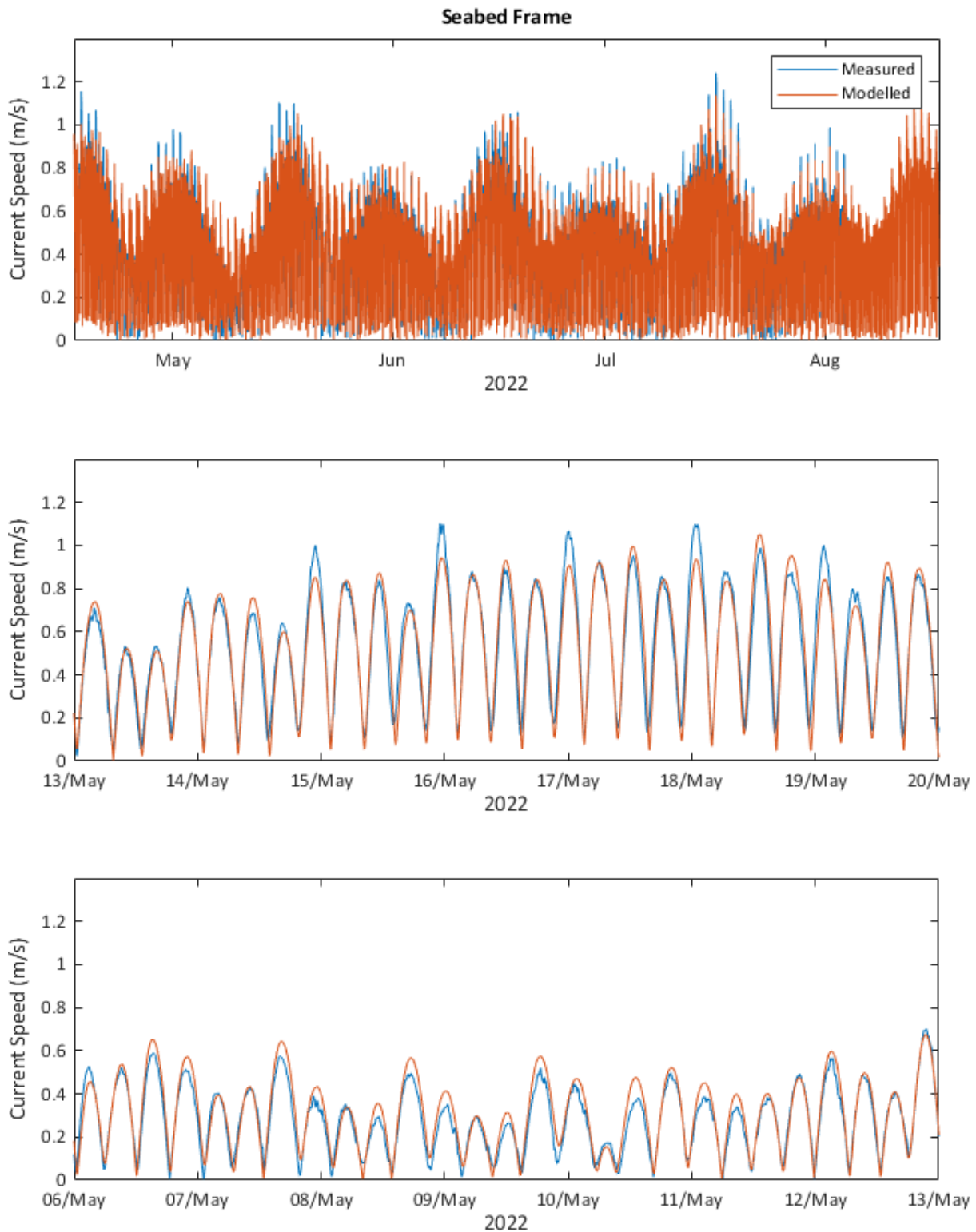


Figure 4.10: Time-series comparison of modelled and measured depth-average current speeds, the Project Seabed Frame.



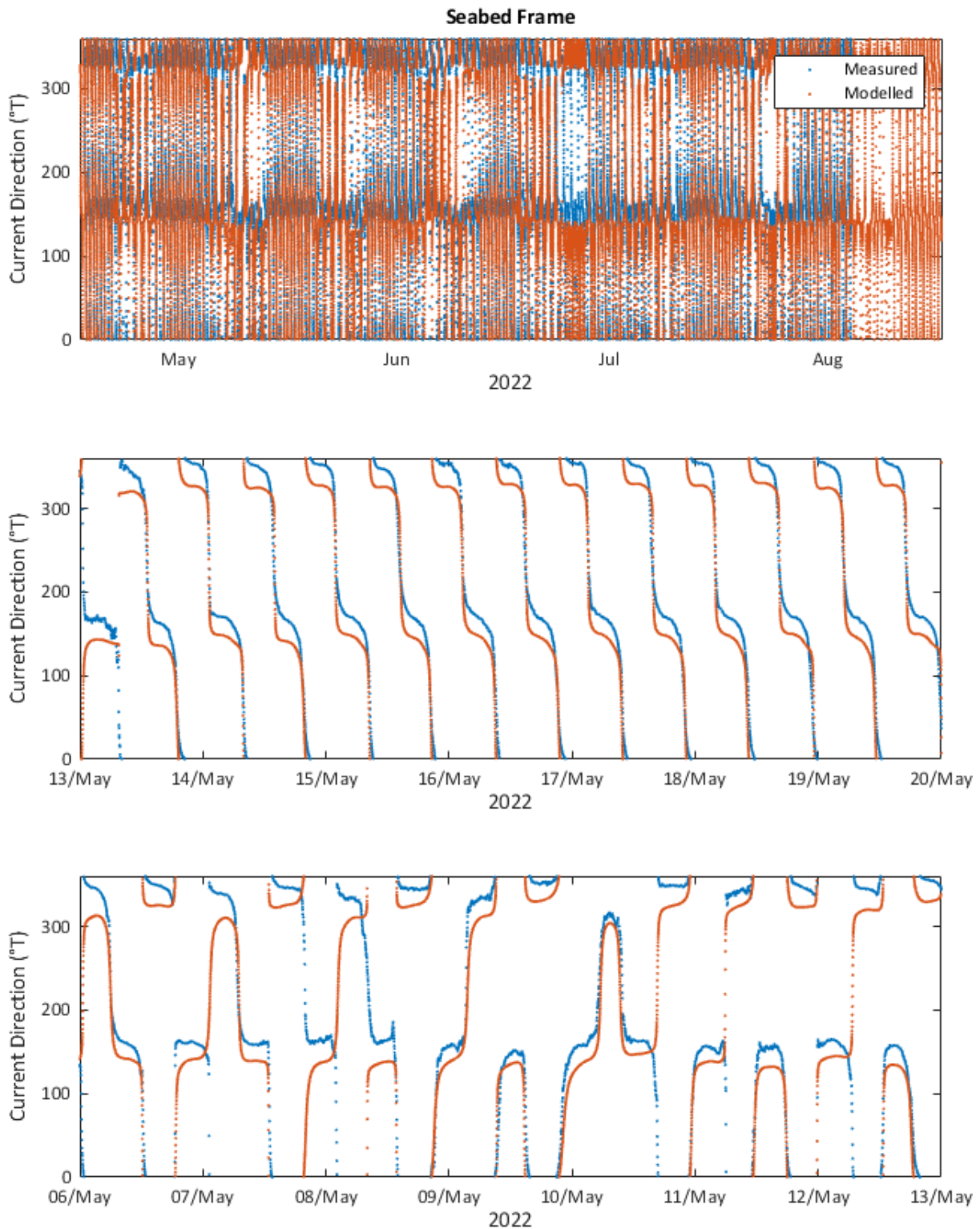


Figure 4.11: Time-series comparison of modelled and measured depth-average current directions, the Project Seabed Frame.

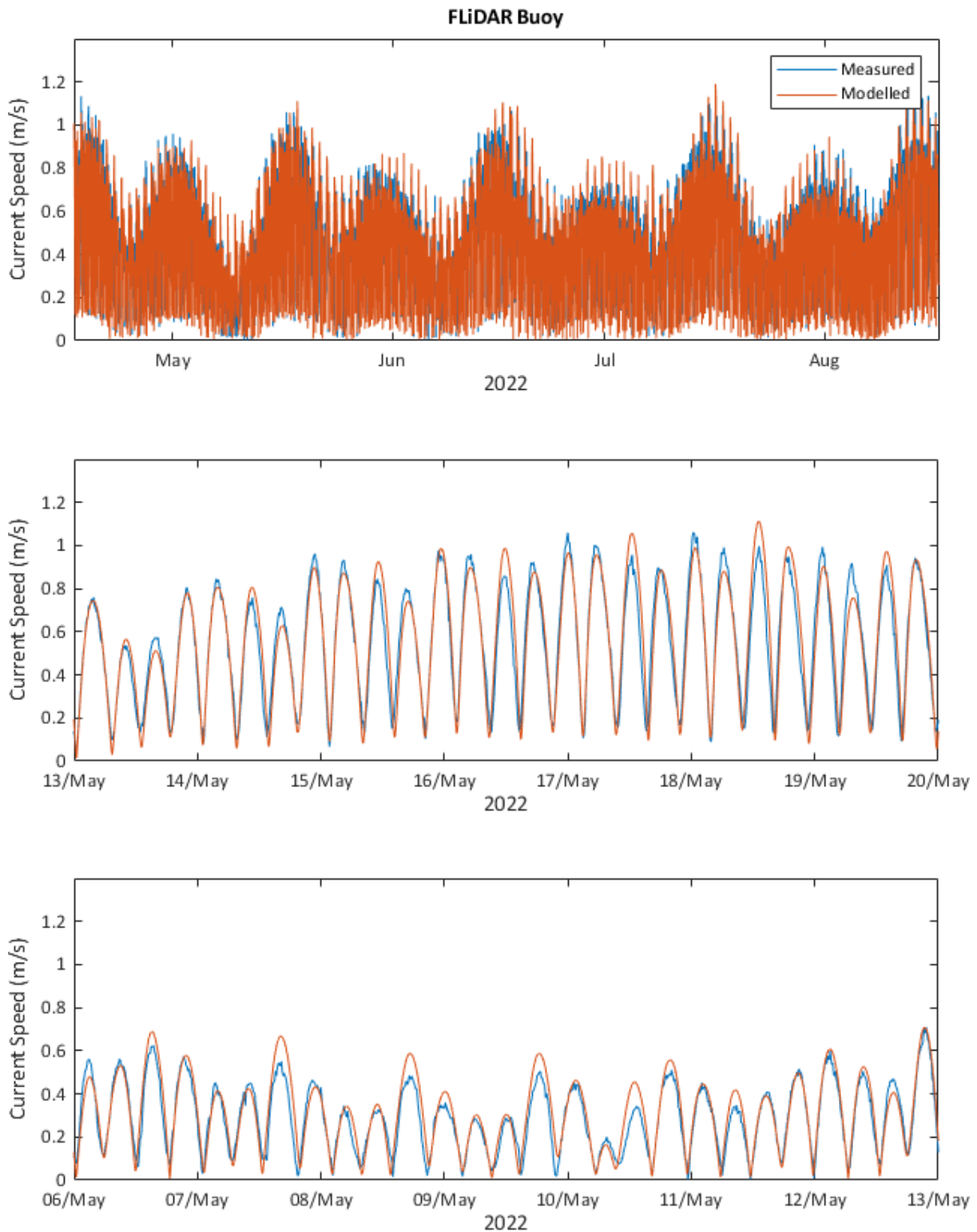


Figure 4.12: Time-series comparison of modelled and measured depth-average current speeds, the Project FLS.

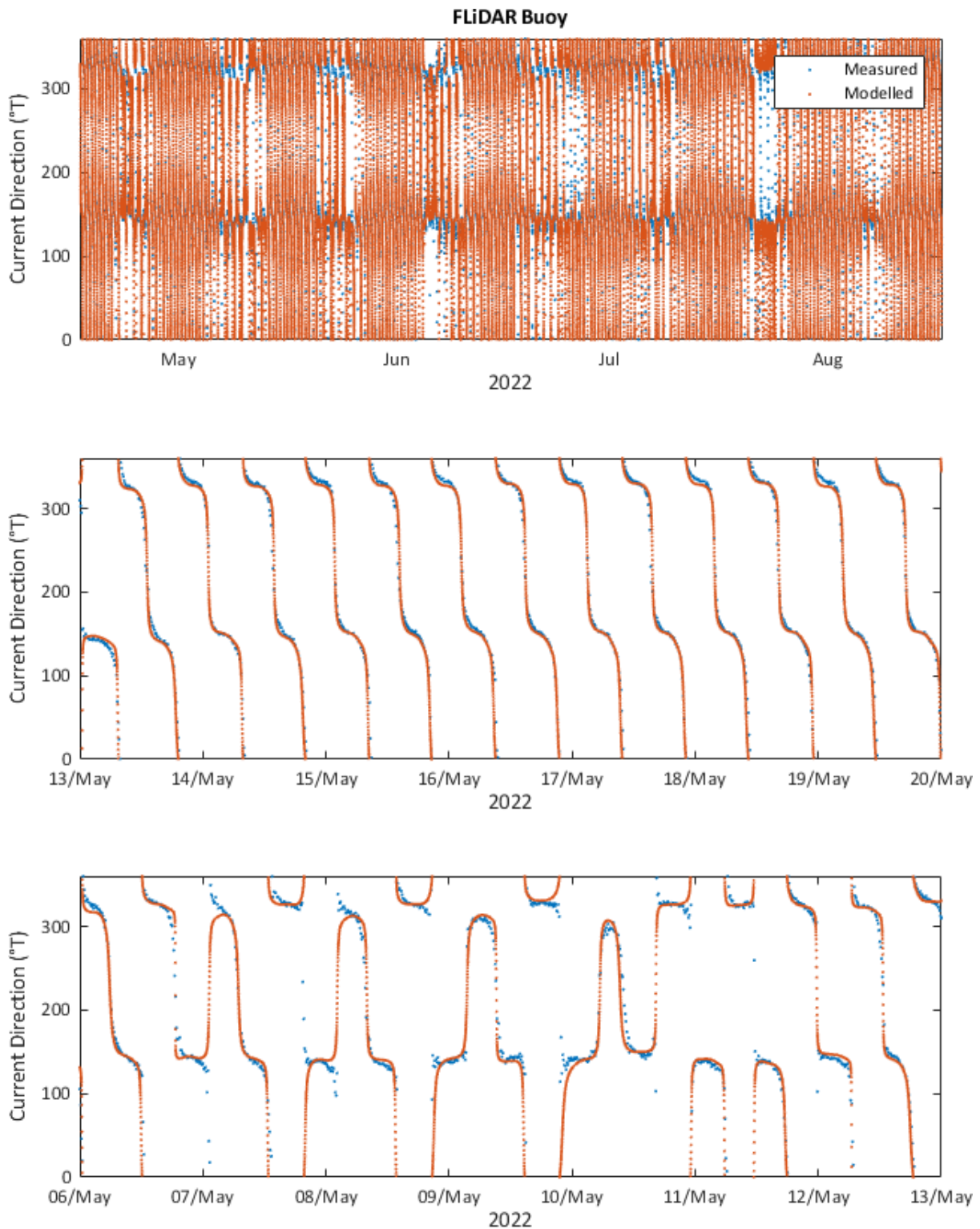


Figure 4.13: Time-series comparison of modelled and measured depth-average current directions, the Project FLS.

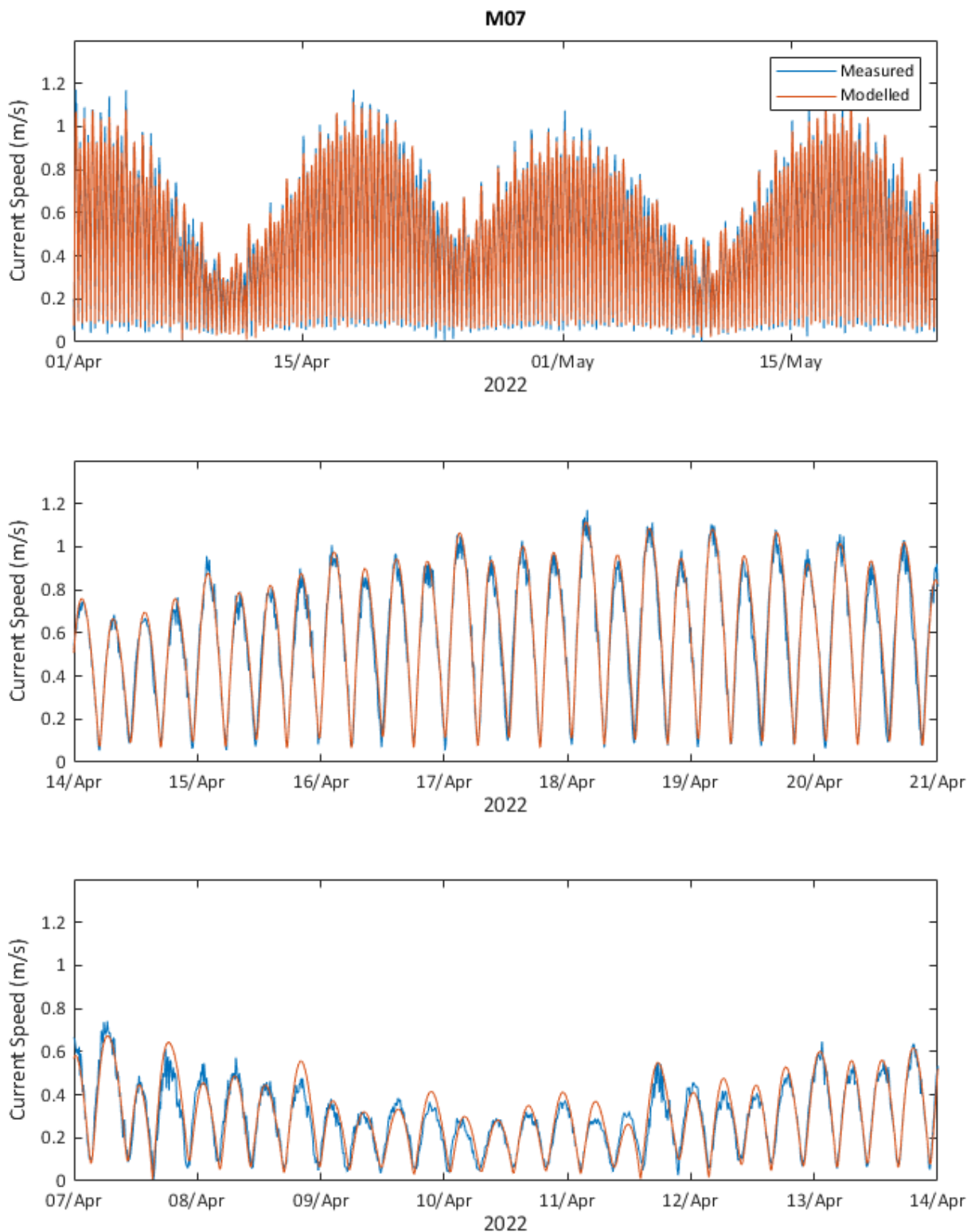


Figure 4.14: Time-series comparison of modelled and measured depth-average current speeds, M07 Seabed Frame.



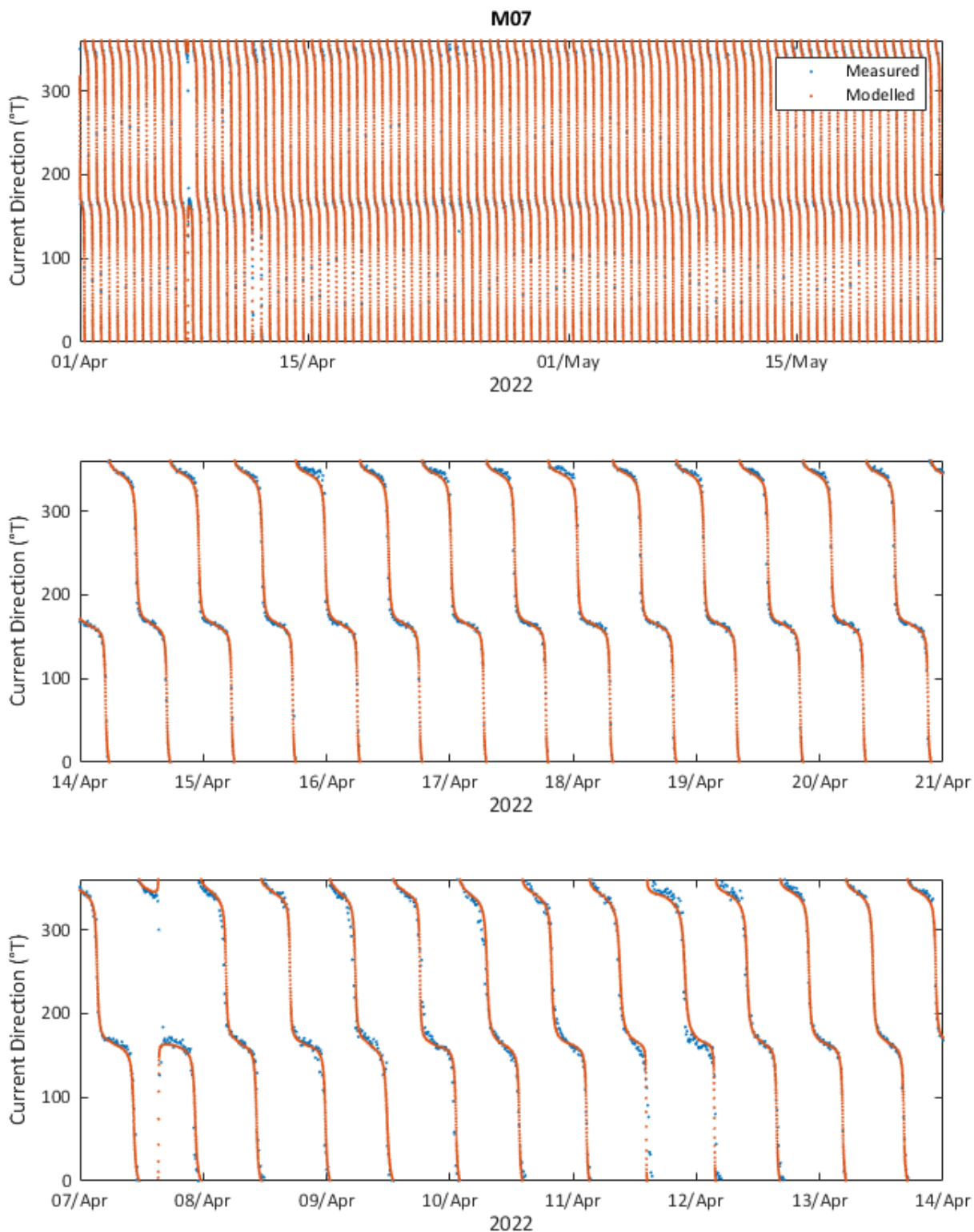


Figure 4.15: Time-series comparison of modelled and measured depth-average current directions, M07 Seabed Frame.



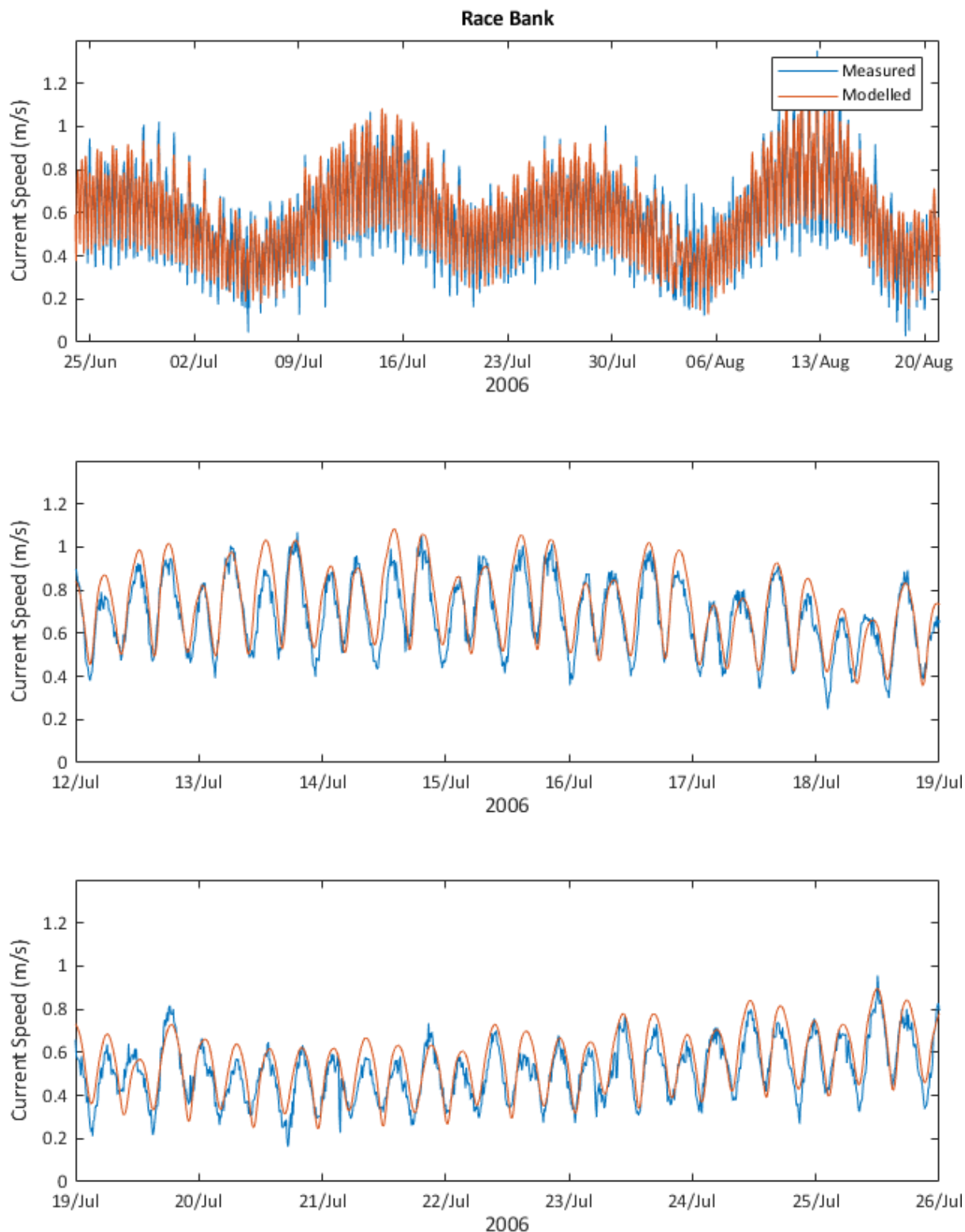


Figure 4.16: Time-series comparison of modelled and measured depth-average current speeds, Race Bank.

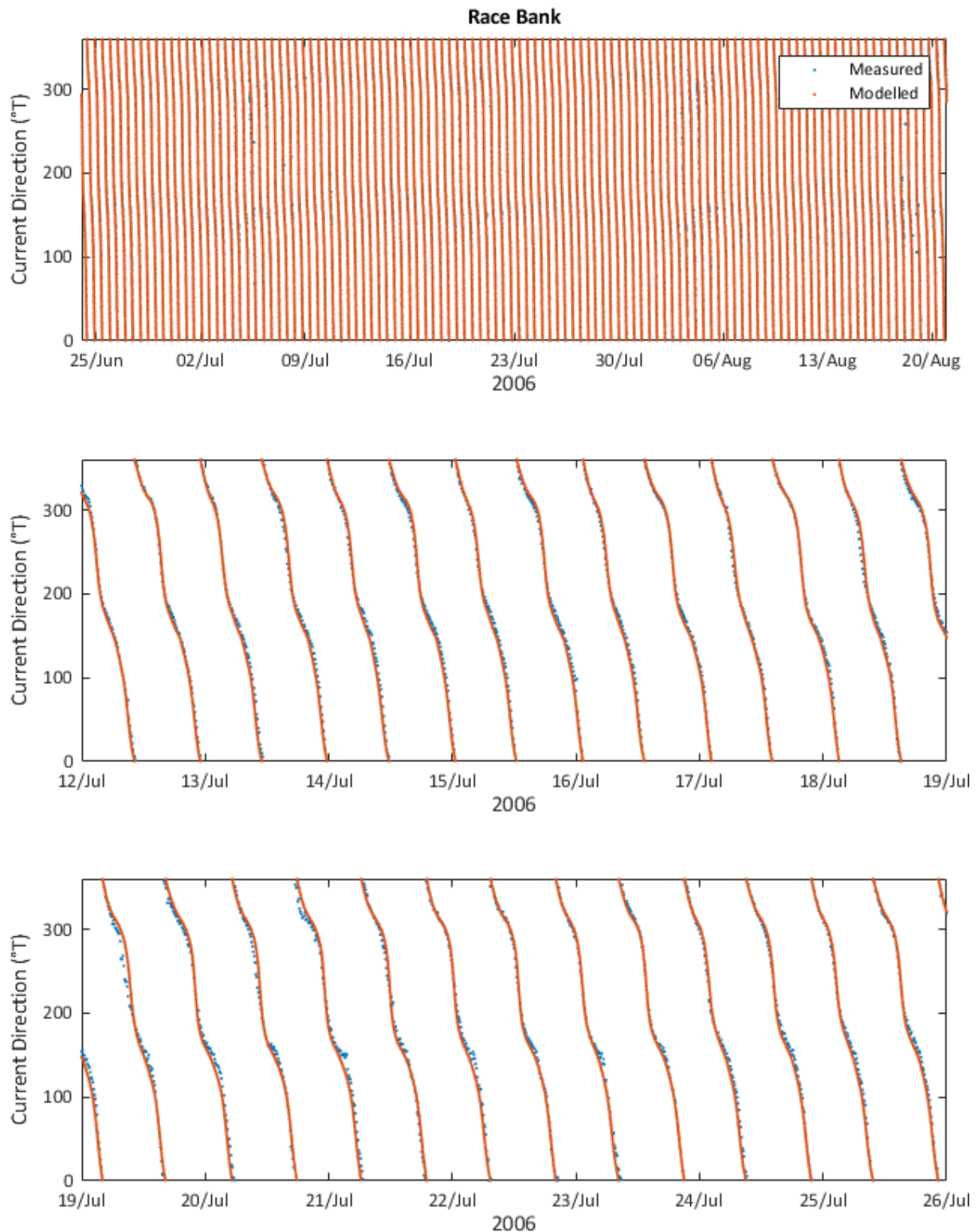


Figure 4.17: Time-series comparison of modelled and measured depth-average current directions, Race Bank.

In general, the model performs best against the measurements from within the array area, and at the M07 location further to the north. Performance is slightly degraded at the Race Bank location inshore, close to the ECC, where the model overpredicts current speeds by around 6% on average (although the very highest current



speeds are still well represented at this location). Nonetheless, the direction and phasing of the tide are both extremely well predicted by the model at Race Bank.

#### 4.5 Selection of Tidal Events

Four tidal events were selected for modelling of hydrodynamic blockage and for particle tracking modelling to encompass the largest (spring) and smallest (neap) likely tidal advection pathways on both flood (southerly) and ebb (northerly) phases of the tide. These were:

Table 4.2: Events selected for hydrodynamic modelling.

Event Name	Description	Date and Time
Peak Spring flood	Flood (southerly) current speed that would be exceeded approximately three times per year (therefore in the top 0.5% of flood current speeds)	30-Sep-2015 11:40
Peak Neap flood	Flood (southerly) current speed that would not be exceeded approximately three times per year (therefore in the bottom 0.5% of flood current speeds)	26-Oct-2005 18:20
Peak Spring ebb	Ebb (northerly) current speed that would be exceeded approximately three times per year (therefore in the top 0.5% of ebb current speeds)	29-Sep-2015 16:40
Peak Neap ebb	Ebb (northerly) current speed that would not be exceeded approximately three times per year (therefore in the bottom 0.5% of ebb current speeds)	26-Oct-2005 23:40

#### 4.6 Hydrodynamic Blockage Modelling

To assess the effect of the presence of the built windfarm on flows and water levels, blockage modelling was used. Blockage modelling uses a sub-grid scale parameterisation of each structure to represent the array-scale blockage to flows caused by the windfarm. The particular windfarm scenario that was modelled is defined in Annex A [1]. Three different structure types were modelled: gravity bases (pertaining to 50% of the WTGs, the ANSs and the ORCPs), offshore sub-stations (OSSs), and suction-bucket jackets (pertaining to the other 50% of the WTGs). The MIKE21 FMHD software allows the user to provide a description of the geometry of the structure in terms of its geographical position, plan shape, height and width, over any number of vertical sections. The model then uses a simple drag law to capture the increasing resistance imposed by the structures as the flow speed increases.

The model was run for the four tidal events described in Table 4.2 to establish a baseline condition. The model was then re-run for the same conditions, but this time including the representation of the windfarm structures. The difference between these two results was calculated for each of the events, providing the predicted difference in flow speeds and water levels caused by the presence of the windfarm.



## 5 Waves

Waves were modelled using a Southern North Sea SWAN model in conjunction with a higher resolution nested model of the Greater Wash. SWAN cycle III version 40.91ABC [8] was used.

Model parameters should be considered as representative of a three-hour sea-state.

### 5.1 Measured Wave Data

To support calibration and validation of the wave model, measured data were acquired from Cefas, the National Network of Regional Coastal Monitoring Programmes of England (NNRCMP), and the World Meteorological Organisation (WMO). The Cefas and Channel Coastal Observatory measurements originate from a Datawell Directional Waverider MkIII, are within the windfarm boundary and are in excess of 15 years in duration. As such, they provide a valuable set of high-quality and long-term measurements against which to calibrate and validate the wave model(s). Details of these datasets are provided in Table 5.1 below and illustrated in Figure 5.1 overleaf.

Table 5.1: Measured datasets used for wave model validation.

Dataset	Provider	Location	Time Period	Water Depth [mLAT]
Chapel Point	NNRCMP	53.2448°N, 0.4470°E	04-Sep-2012 to Near Present	13m
Dowsing	Cefas	53.5318°N, 1.0538°E	06-Oct-2003 to 02-Sep-2020	22m
West Sole	WMO	53.7000°N, 1.1500°E	01-Jan-1979 to 17-Oct-1990	21m

The measurements were carefully reviewed prior to use. In terms of performance, data from Dowsing and Chapel Point Datawell Waverider buoys were considered to be of the highest quality owing to the modern instrumentation used in the measurements. They are also geographically closest to the Project array area and export cable route.

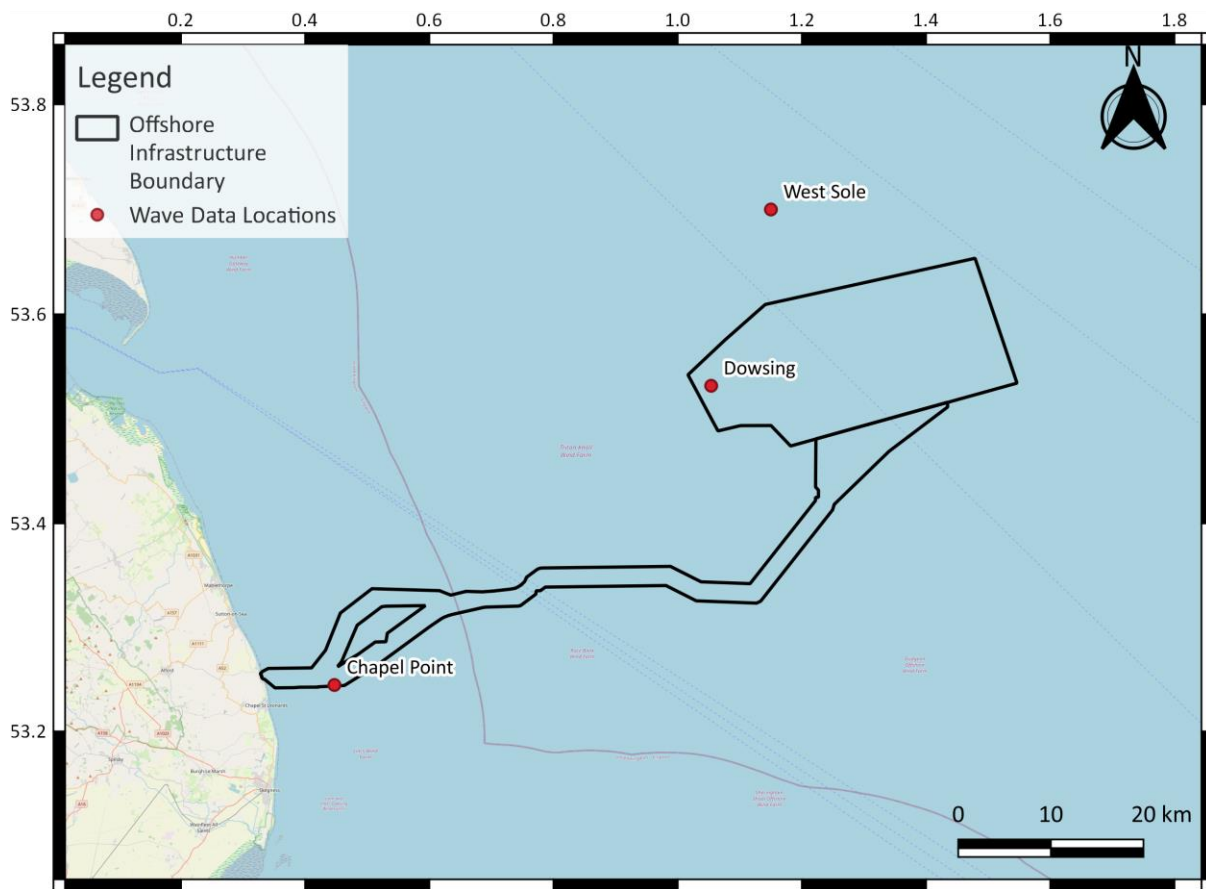


Figure 5.1: Locations of the wave measurement devices.

## 5.2 Modelling Software

A bespoke SWAN wave model was applied to help assess wave blockage effects due to the windfarm. SWAN is a third-generation wave model, developed at Delft University of Technology, which computes random, short-crested wind-generated waves in coastal regions and inland waters. SWAN accounts for the following physical interactions:

- Wave propagation in time and space, shoaling, refraction due to current and depth, frequency shifting due to currents and non-stationary depth;
- Wave generation by wind;
- Three- and four-wave interactions;
- White-capping, bottom friction and depth-induced breaking;
- Wave-induced set-up;
- Transmission through and reflection (specular and diffuse) against obstacles, and;
- Diffraction approximation.

For model validation, a large-scale regional model was deployed with a spatial resolution of 10km whilst the nested high-resolution local model used a horizontal resolution of 200m which covers the array and ECC area.



## Marine Physical Processes – Numerical Modelling

The large-scale model takes boundary wave spectra from the ERA5 model described in Section 5.3, and then generates boundary spectra for the high-resolution model. The wave model extents are described in Table 5.2, and shown in Figure 5.2 below.

Table 5.2: Wave model domains.

Wave Model	Geographical Extents
10km Wave Model	50.9584°N, 3.09°W to 56.0417°N, 6.09°E
200m Wave Model	52.8 °N, 0.4°W to 54.2°N, 1.6°E

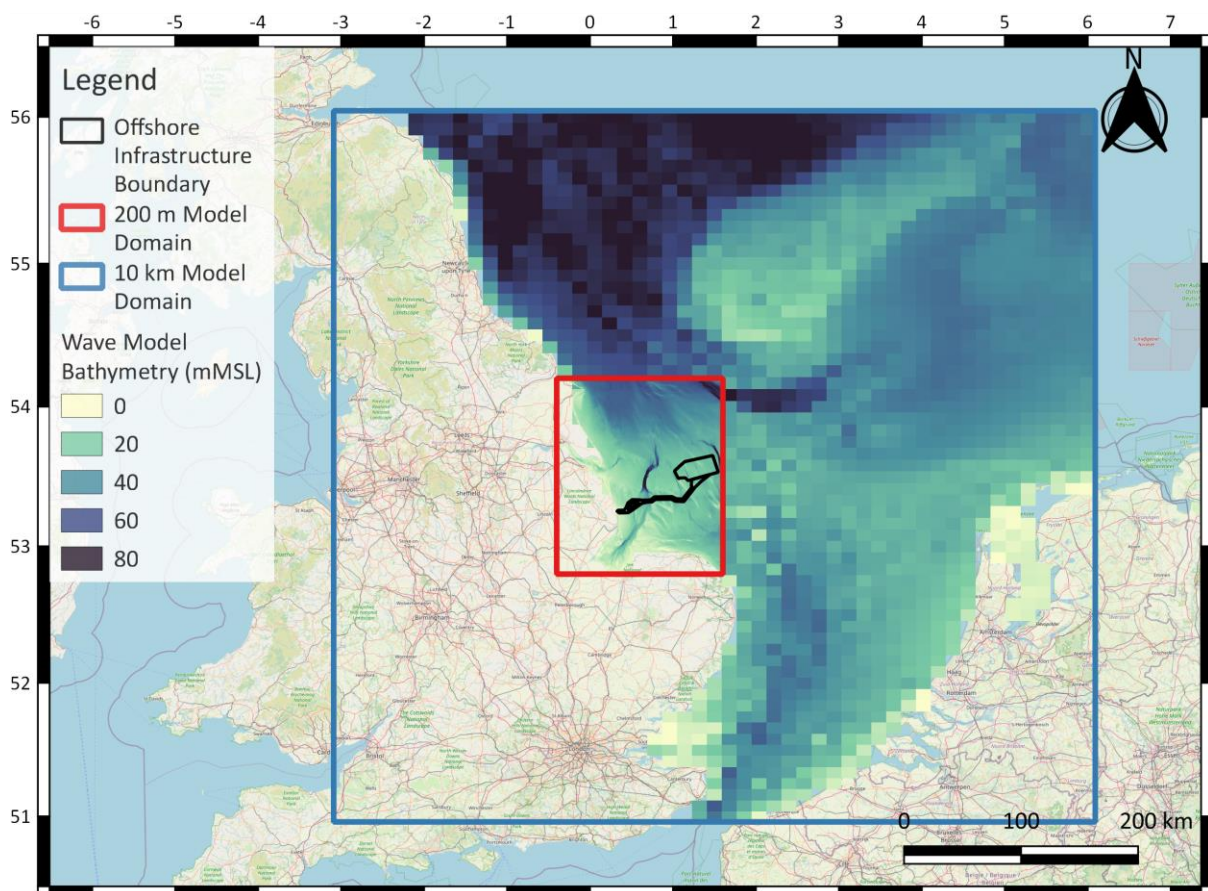


Figure 5.2: Wave model domains.

For the wave blockage modelling, the large-scale regional model was not used and instead the high-resolution local model was driven at its boundaries with parameters specified to create the desired conditions at the windfarm.

### 5.3 Model Boundary Conditions

Spectral wave boundary conditions to the large domain 10km model originated from ECMWF ReAnalysis 5 (ERA5). ERA5 incorporates a model with three fully-coupled components for the atmosphere, land surface, and ocean waves. The wave model is based on the Wave Analysis Model (WAM) approach (Komen et al, 1994 [9]). The horizontal resolution of the output wave data is 0.5° (approximately 56km in latitude and 30km in longitude



in the region of interest) and wave spectra are discretised using 24 directions and 30 frequencies from 0.0345 to 0.5473Hz. Data are available every hour between 1979 and present. MetOceanWorks adjusted ERA5 wind fields (see Section 3.3) were applied to the sea surface at hourly intervals.

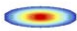
## 5.4 Model Validation


The wave model has been extensively validated against the measured wave data detailed in Table 5.1 with pertinent results presented in the following pages. These assessments demonstrate good model skill in terms of wave height and period under both ambient and storm conditions. Scatter plots with overlaid Quantile-Quantiles are presented and generally yield high correlation coefficients, relatively low scatter indices and slopes close to unity.


Care has been taken when comparing mean zero-crossing periods ( $T_{m02}$ ) to ensure both modelled and measured values are derived using the same method. Parameters derived from higher order spectral moments, such as  $T_{m02}$ , can be somewhat sensitive to how high frequency wave energy is treated in their derivation. In particular, for the Dowsing and Chapel Point datasets,  $T_{m02}$  as output directly from the SWAN model *does* make use of a theoretical high frequency extrapolation, whilst that reported by the Dowsing and Chapel Point DWR measurements does *not*. Direct comparison of these parameters can be misleading, the inclusion of such a tail generally being expected to reduce the  $T_{m02}$  values. In order to more fairly compare, modelled  $T_{m02}$  have been recalculated from modelled *spectra*, without including a high frequency extrapolation and instead using the same high frequency cut-off as the DWR measurements. It is these modelled values which are compared to the measured  $T_{m02}$  below.




Mean (X)	1.19
Mean (Y)	1.22
N	97552
Bias	0.03
AME	0.16
RMS	0.20
SI	0.17
CC	0.96
R <sup>2</sup>	0.92

**Data** 

**1:1 Line** 

**Quantiles (1-99%)** 

**Q-Q Line: 1.001x** 

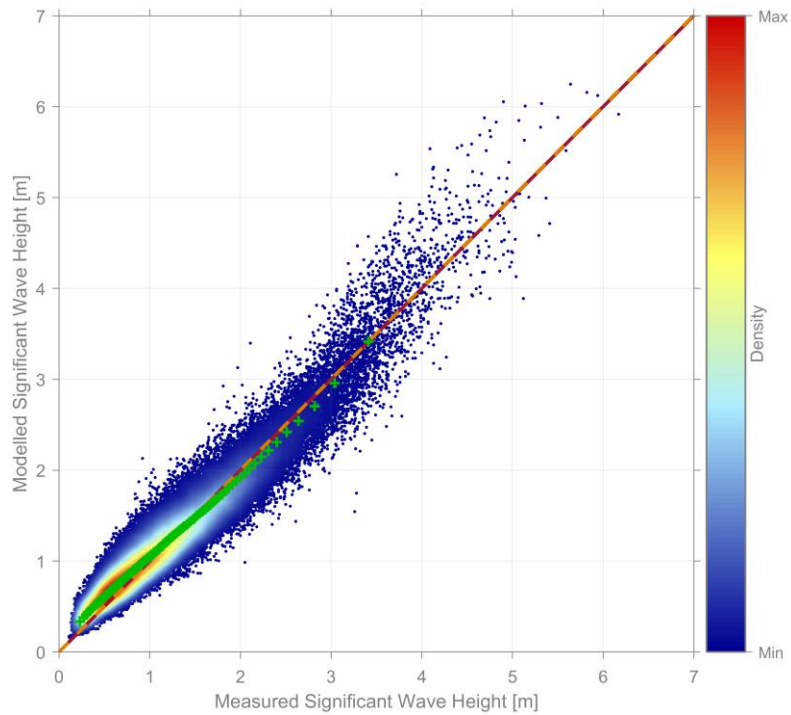
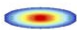





Figure 5.3. Outer Dowsing, Hm0 validation, all data.

Mean (X)	6.53
Mean (Y)	6.53
N	85205
Bias	-0.00
AME	0.86
RMS	1.54
SI	0.24
CC	0.77
R <sup>2</sup>	0.59

**Data** 

**1:1 Line** 

**Quantiles (1-99%)** 

**Q-Q Line: 0.986x** 

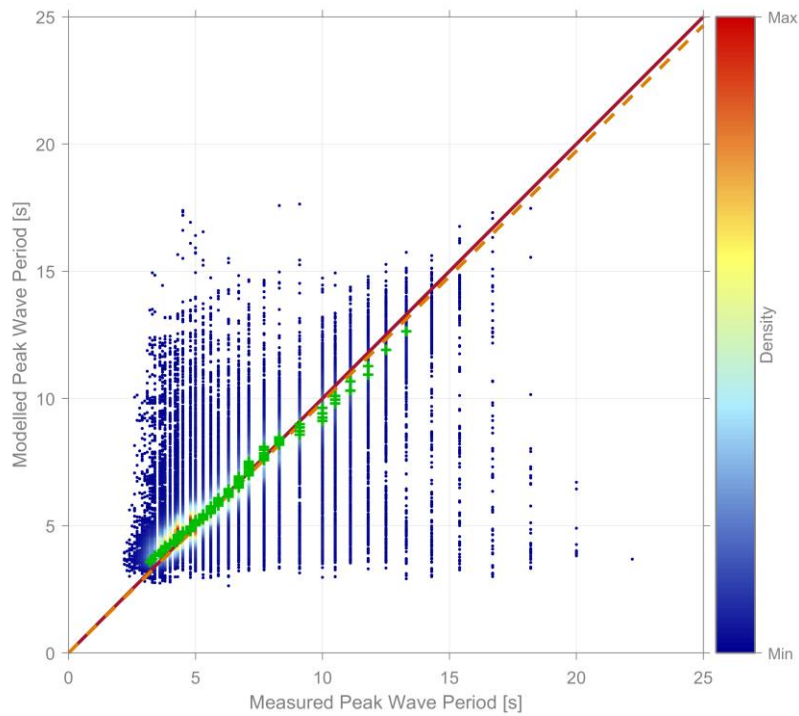


Figure 5.4. Outer Dowsing, Tp validation, all data.



Mean (X)	4.27
Mean (Y)	4.35
N	100354
Bias	0.08
AME	0.36
RMS	0.48
SI	0.11
CC	0.87
R <sup>2</sup>	0.75

Data	
1:1 Line	
Quantiles (1-99%)	
Q-Q Line: 1.019x	

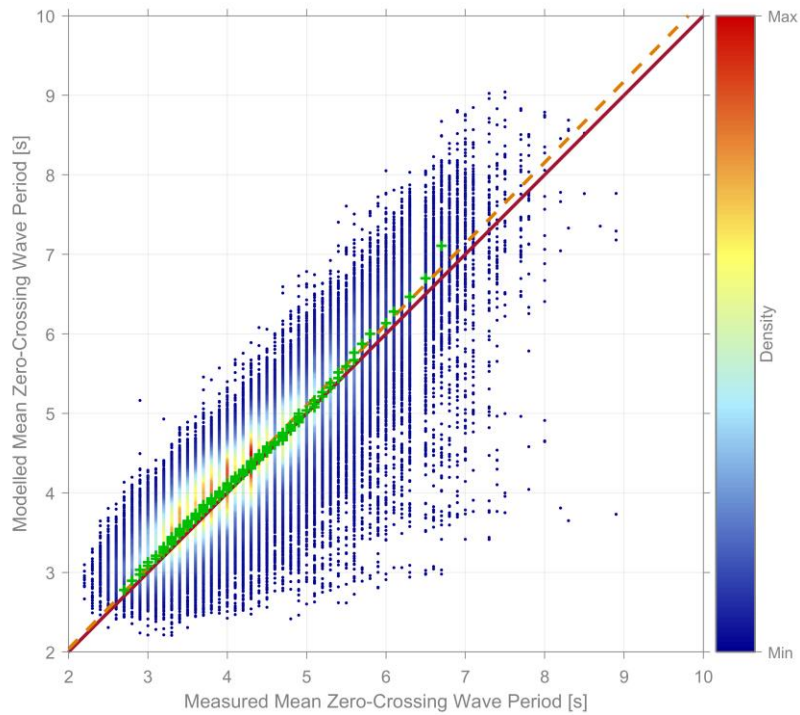


Figure 5.5. Outer Dowsing, Tm02 validation, all data.

Mean (X)	0.77
Mean (Y)	0.86
N	75202
Bias	0.09
AME	0.14
RMS	0.18
SI	0.21
CC	0.93
R <sup>2</sup>	0.87

Data	
1:1 Line	
Quantiles (1-99%)	
Q-Q Line: 1.077x	

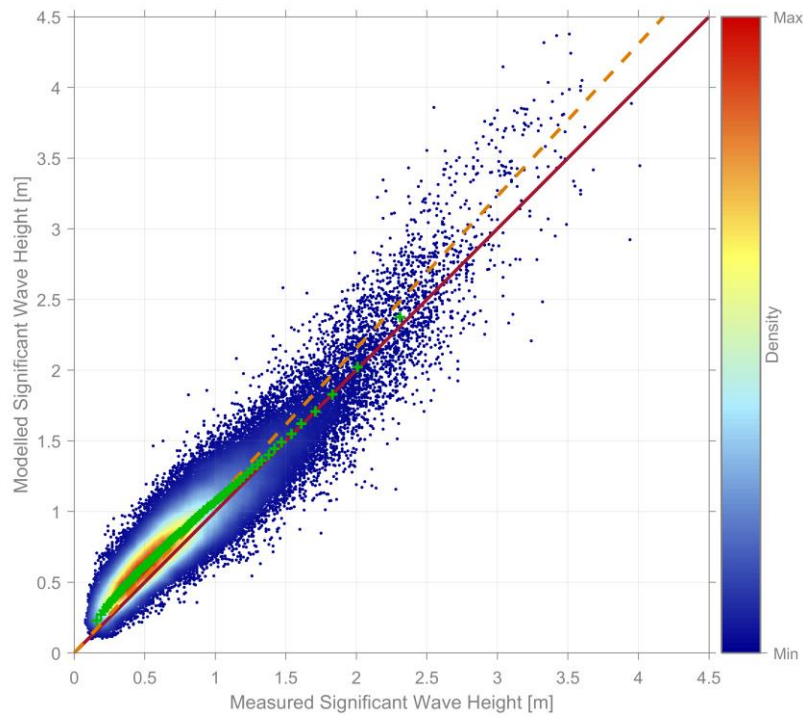
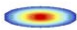



Figure 5.6. Chapel Point, Hm0 validation, all data.









Mean (X)	6.24
Mean (Y)	6.08
N	52861
Bias	-0.16
AME	1.08
RMS	1.87
SI	0.30
CC	0.74
R <sup>2</sup>	0.55

**Data** 

**1:1 Line** 

**Quantiles (1-99%)**   

**Q-Q Line:**  **0.948x**

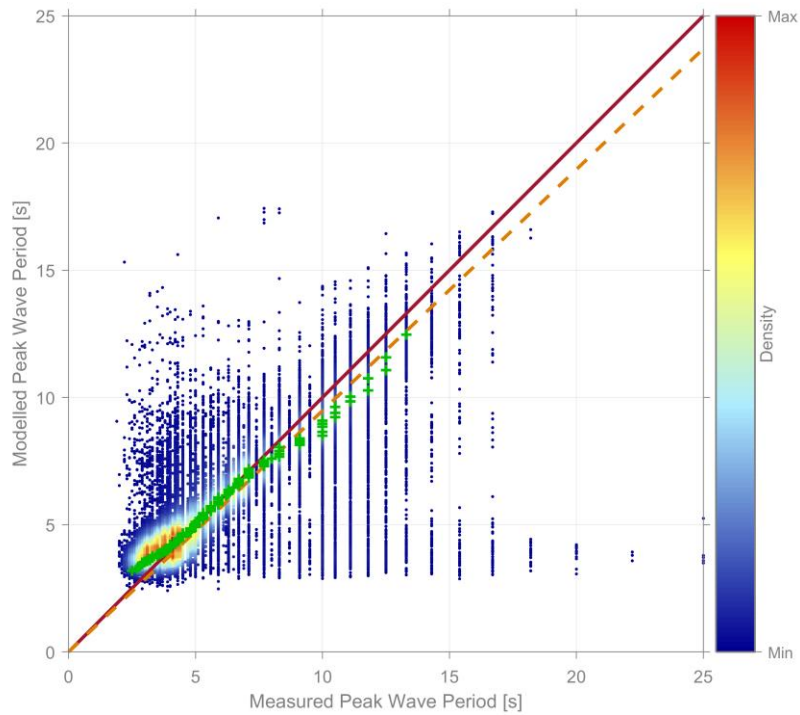
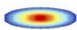







Figure 5.7. Chapel Point, Tp validation, all data.

Mean (X)	3.77
Mean (Y)	3.72
N	75202
Bias	-0.05
AME	0.42
RMS	0.58
SI	0.15
CC	0.78
R <sup>2</sup>	0.61

**Data** 

**1:1 Line** 

**Quantiles (1-99%)**   

**Q-Q Line:**  **0.979x**

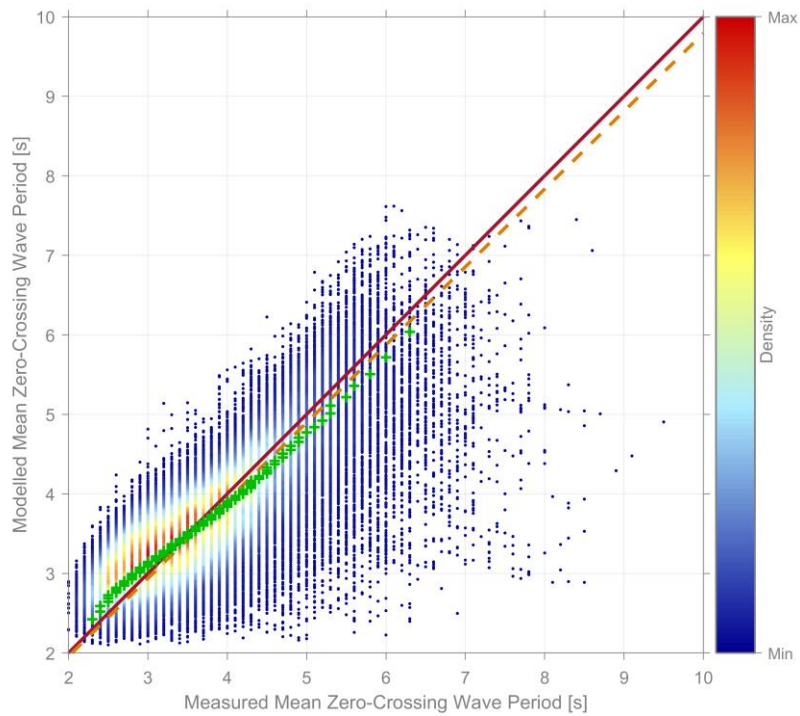


Figure 5.8. Chapel Point, Tm02 validation, all data.





## 5.5 Selection of Wave Events

The wave model was run for three event magnitudes – p50 (median) waves, and 1 in 1 and 1 in 100 year extreme waves, originating from two directions - north east, and north. The high-resolution model boundary conditions (input wind speed and wave parameter boundaries) were adjusted such that conditions at the CENTRAL location within the array matched the following conditions as defined in the Project metocean design criteria report [10] at the 'CENTRAL' location.

Table 5.3: Wave conditions modelled.

Event Name	Direction [°N from]	Hm0 [m]	Tp [s]
P50	45	1.0	5.4
1 in 1	45	4.4	10.3
1 in 100	45	6.9	12.7
P50	0	1.2	5.7
1 in 1	0	5.1	11.0
1 in 100	0	8.1	13.8

## 5.6 Wave Blockage Modelling

To assess the array-scale effect of the presence of the built windfarm on waves, blockage modelling was used. Blockage modelling uses a sub-grid scale representation of each foundation structure to represent the blockage to waves caused by the windfarm. The particular windfarm scenario that was modelled is defined in Annex A [1]. Three different structure types were modelled: gravity bases (pertaining to 50% of the WTGs, the ANSs and the ORCPs), offshore sub-stations (OSSs), and suction-bucket jackets (pertaining to the other 50% of the WTGs). The SWAN software allows the user to provide a description of the structure as a coefficient of transmission through specified model grid cells (in this case, the cells containing the structures).

After a run of the model with no structures represented, the model was then re-run for the same conditions, but this time including the representation of the windfarm foundation structures. The difference between these two results was calculated for each of the events, providing the predicted difference in wave conditions caused by the imposition of the windfarm.



## 6 Particle Tracking

The Particle Tracking module of MIKE 21 Flow Model FM (Flexible Mesh) is used for modelling the transport and fate of suspended and sedimented substances discharged in estuaries and coastal areas or in the open sea. The material is considered as particles forming a sediment plume being advected with the surrounding water body and dispersed as a result of random (turbulent) processes in three dimensions. The particles settle with a constant settling velocity. A mass is attached to each particle. The following processes are attached to individual particle classes:

- Settling;
- Moving sources (if applicable); and
- Horizontal and vertical dispersion.

The model calculates the path of each particle and outputs the instantaneous concentrations of individual classes in two dimensions, as well as the settled mass. The output concentration is based on the mass of particles present in the volume of water in a given model cell. The settled mass is converted to a deposition depth by dividing by the settled density of the material under consideration. For the purpose of the present assessment, re-erosion of settled material is not considered to ensure a conservative level of deposition.

The hydrodynamic model (and therefore the output grid) had a spatial resolution featuring a triangular mesh with 200m resolution in the Project development area and surrounds. The Project required that material concentrations as low as 1mg/l above background were resolved. Given that some releases are modelled near to the shallow coastal waters (for instance, Bentonite release), the model was also required to resolve these minimum concentrations in areas of relatively shallow water. A cut-off depth of 1.5m was chosen for resolving the minimum required concentrations in the model. Assuming that the triangular mesh is composed of triangles tending toward an equilateral shape, and a water depth corresponding with mean sea level, the volume of water in an individual mesh element with water depth 1.5m is 60,026m<sup>3</sup>. In order to resolve to 1mg/l in this volume of water, each particle must have a maximum mass of 60kg. Therefore, a sufficiently high number of particles was released in each run such that each particle was assigned a maximum mass of 60kg in the model. Although each particle has representative maximum mass 60kg, it inherits the settling velocities of its class from Table 1 of Annex A [1]. The relevant part of the table is reproduced here as Table 6.1.

Table 6.1: Details of the representative sediment types.

Sediment type	Size range (mm)	Representative size (mm)	Settling velocity (m/s)
Fine sand	0.125 to 0.250	0.188	0.018
Very fine sand	0.063 to 0.125	0.094	0.005
Coarse silt	0.031 to 0.063	0.047	0.0014
Medium silt / muds	< 0.0031	0.023	0.0003

Coarser sediment types with a faster settling velocity are not considered in the particle model as they will fall to the seabed relatively quickly and not be subject to wider advection or dispersion to form part of any sediment plume. Where coarse sediments are released remote from their point of origin (such as spoil disposal) then their fate is considered separately (i.e., Annex B [2] for spoil mounds).

Brief details of the model set up for each of the scenarios follows. More details of realistic worst-case scenarios that these are based on can be found in Annex A [1]. As described in Section 4.5, for each scenario, four different current events were simulated. These are high and low current speeds, flowing northward (ebb) and southward (flood). The geographical positions of each of the locations described below is shown in Figure 6.1.

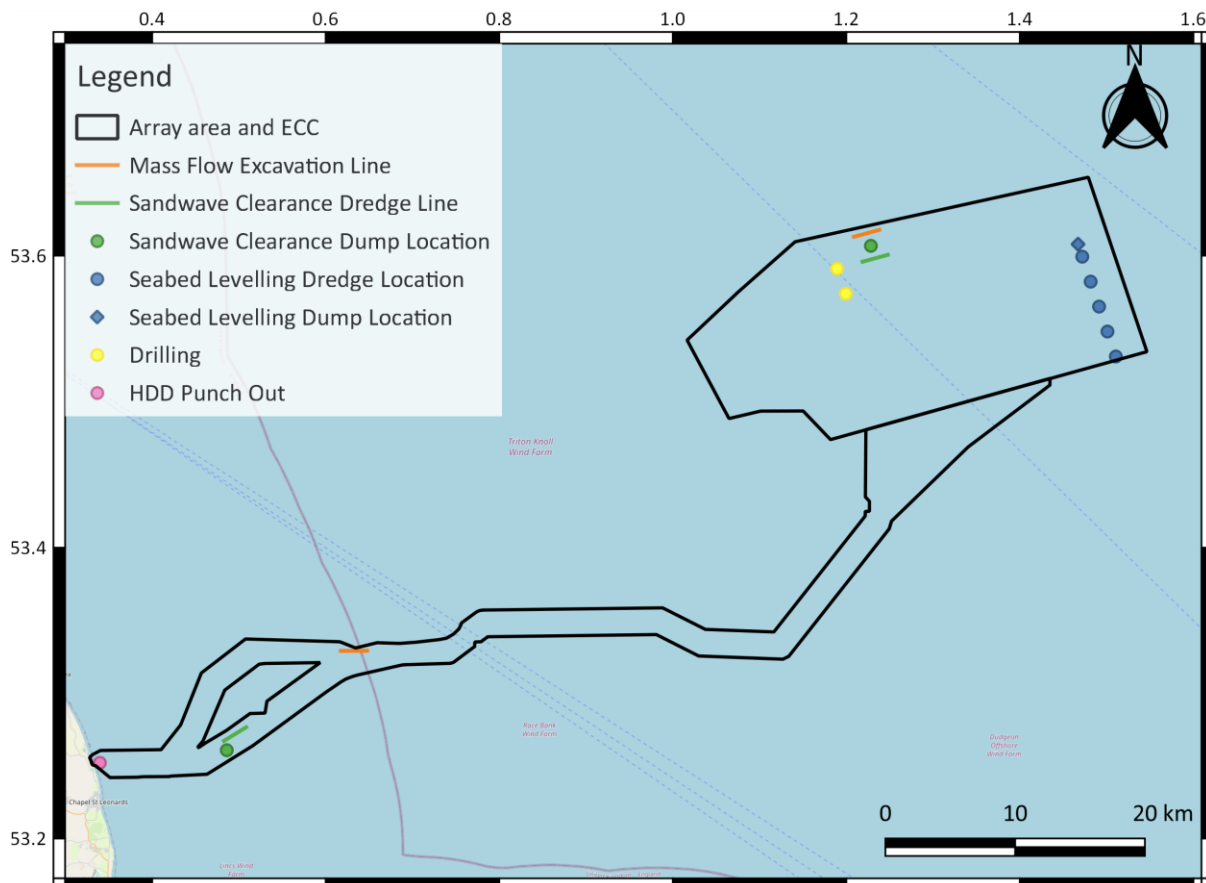


Figure 6.1. Locations used in particle tracking modelling.

## 6.1 Array Area

### 6.1.1 Inter Array Cabling – Mass Flow Excavator Trenching

The mass flow excavator is simulated to be moving along the line from WTG 9 to 10 at a rate of 215m per hour, meaning that the trenching between these two WTGs is expected to take around nine hours. In each case, the excavation is simulated to start just over two hours before the current speed peak, meaning that the current speed peak events occur approximately a quarter of the way along the excavation route. The material is released into the model at 2.5m above the bed (the height above the bed is taken to be equivalent to the depth of the trench produced by the mass flow excavator). To convert the settled mass from the model into a depth in mm, a settled density of  $1,168\text{kg/m}^3$  was used. All settled densities in this study were calculated using the proportion of fine sands versus the proportion of medium silts / muds in the sediments for each scenario, and proportionally



assigning commonly-accepted densities for fine sands ( $1,430\text{kg/m}^3$ ), and for medium silts / muds ( $200\text{kg/m}^3$ ) to the settled material (see [11]).

### **6.1.2 Inter Array Cabling – Sandwave Clearance**

Six TSHD hopper loads are simulated as being filled (including overspill discharges) along the cable route between WTG20 and WTG21, and then discharged at an adjacent dump site approximately 1km to the north (in between adjacent WTG locations). During filling, the TSHD is simulated as moving at a speed of 1m/s. Assuming a required clearance width of 30m, the TSHD travels along the entire length of the 2km line, before discharging the hopper. The TSHD then picks up where it left off and continues to dredge back and forth along the line, discharging the hopper after each completion of the line. The overspill phase from the TSHD lasts one hour. There is then a 25-minute break in discharge during demob and transit to the dump site, before a 10-minute dumping period at the dump site. There is then a 55-minute break before overspill begins again which accounts for the initial loading period. The current speed peaks occur 15 minutes after the end of the third dumping phase. For the overspill phase the material is released into the model at the water surface, and for the dumping phase the material is released 12 m below the surface. To convert the settled mass from the model into a depth in mm, a settled density of  $1,217\text{kg/m}^3$  was used.

### **6.1.3 Foundation Installation – Drilling**

Two locations for drilling are simulated at OSP101 and at WTG79, with both locations being drilled simultaneously. The release of drill arisings is simulated to persist for 24.5 hours, with the current speed peak occurring 3.5 hours into the release period. During the release period, the initial release of overburden is simulated to last for around 3.5 hours, before release of material from the rock layer continues for the rest of the drilling period (around 21 hours).

To convert the settled mass from the model into a depth in mm, a settled density of  $266\text{kg/m}^3$  was used for the overburden, and  $1,184\text{kg/m}^3$  for the rock layer.

### **6.1.4 Foundation Installation – Bed Levelling**

A single TSHD hopper load is simulated as being filled (including overspill discharges), and then discharged at an adjacent dump site. The foundation sites simulated being levelled are WTG65, 58, 50, 95 and 94, and the dump site is north of WTG94, midway to WTG93 (in between adjacent WTG locations). The overspill phase from the TSHD lasts one hour, therefore occurring at WTGs 50, 95 and 94. There is then a 5-minute break in discharge during demob and transit to the dump site, before a 10-minute dumping period at the dump site. The current speed peaks occur at the beginning of the dumping phase. For the overspill phase the material is released into the model at the water surface, and for the dumping phase the material is released 12 m below the surface. To convert the settled mass from the model into a depth in mm, a settled density of  $1,172\text{kg/m}^3$  was used.

## **6.2 Export Cable Route**

### **6.2.1 HDD Punch-out - Bentonite Release**

A single location for HDD punch-out and associated Bentonite release is simulated. The location is approximately 600m from shore in the centre of the cable corridor. The release of Bentonite is simulated to last for 12 hours (initial punch-out followed by a reaming phase), with the current speed peak occurring half way through the release period. To convert the settled mass from the model into a depth in mm, a settled density of  $100\text{kg/m}^3$  was used.



### 6.2.2 Sandwave Clearance

Six TSHD hopper loads are simulated as being filled (including overspill discharges) along a section of the cable corridor approximately 11km offshore, and then discharged at an adjacent dump site approximately 1km to the south. During filling, the TSHD is simulated as moving at a speed of 1m/s. Assuming a required clearance width of 30m, the TSHD travels along the entire length of the 2km line, before discharging the hopper. The TSHD then picks up where it left off and continues to dredge back and forth along the line, discharging the hopper after each completion of the line. The overspill phase from the TSHD lasts one hour. There is then a 25-minute break in discharge during demob and transit to the dump site, before a 10-minute dumping period at the dump site. There is then a 55-minute break before overspill begins again. The current speed peaks occur 15 minutes after the end of the third dumping phase. For the overspill phase the material is released into the model at the water surface, and for the dumping phase the material is released 12 m below the surface. To convert the settled mass from the model into a depth in mm, a settled density of 1,148kg/m<sup>3</sup> was used.

### 6.2.3 Mass Flow Excavator Trenching

The mass flow excavator is simulated to be moving along a section of the cable route approximately 22km offshore at a rate of 215m per hour, meaning that the trenching takes nine hours. In each case, the excavation is simulated to start just under three hours before the current speed peak, meaning that the current speed peak events occur approximately a third of the way along the excavation route. The material is released into the model at 2.5m above the bed (the height above the bed is taken to be equivalent to the depth of the trench produced by the mass flow excavator). To convert the settled mass from the model into a depth in mm, a settled density of 946kg/m<sup>3</sup> was used.





## 7 Results

Results from each scenario were provided to GoBe Consultants Ltd in GIS format for interpretation in the relevant EIA chapters. For the results of the wave blockage modelling, raster GeoTIFFs are used, and for all other results, ESRI-format vector shapefiles were used. In the case of the vector shapefiles, all parts of the shapefile where the property is precisely zero, were removed.

- Two output parameters are provided:
  - Sedimented (showing the depth of sediment that has settled on the seabed after release). Note that re-suspension was switched off in the model.
  - Suspended (showing the depth-averaged concentration of sediment that is in suspension after release).
- For each of the four current events, and for each output parameter, the following were provided:
  - The situation at 0, 1, 2, 3, 4, 5, 10, 15 and 20 hours after the beginning of dredge operations
  - The maximum of sedimented and suspended. This represents the largest value that occurred in each model grid cell over the entire 48-hour simulation period. It is not representative of any single instant in time, but does provide a useful indication of the maximal extent of the plume and associated sedimentation. Note that because re-suspension is switched off in the model, the maximum sedimentation is the same as the sedimentation situation at the final model time step.
- The units of 'suspended' are depth-averaged mg/l. The units of 'sedimented' are mm.



---

## References

- [1] Cooper Marine Advisors, “Outer Dowsing Offshore Wind. Annex A: EIA - Determination of Marine Processes Realistic Worst-Case,” Cooper Marine Advisors, 2023.
- [2] Cooper Marine Advisors, “Outer Dowsing Offshore Wind. Annex B: EIA - Assessment of spoil mounds,” Cooper Marine Advisors, 2023.
- [3] The European Marine Observation and Data Network, “Bathymetry | European Marine Observation and Data Network (EMODnet),” The European Marine Observation and Data Network, 01 February 2023. [Online]. Available: <http://www.emodnet-bathymetry.eu>. [Accessed 01 February 2023].
- [4] MetOceanWorks, “Metocean Data Overview - Outer Dowsing Offshore Wind Farm - Export Cable Corridor,” MetOceanWorks, 2023.
- [5] AVISIO, “GLOBAL TIDE - FES,” 01 February 2023. [Online]. Available: <https://www.aviso.altimetry.fr/en/data/products/auxiliary-products/global-tide-fes.html>. [Accessed 01 February 2023].
- [6] DHI, “Mike 21 Flow Model FM: Hydrodynamic Module: User Guide,” DHI A/S, Denmark, 2021.
- [7] DHI, “MIKE 21 Flow Model FM: Hydrodynamic and Transport Module; Scientific Documentation,” DHI A/S, Denmark, 2021.
- [8] SWAN team, Delft University of Technology, “Swan cycle III version 40.91 ABC - Scientific and Technical Documentation,” 2013.
- [9] G. J. Komen, L. Cavaleri, M. Donelan, K. Hasselmann, S. Hasselmann and P. A. E. M. Janssen, Dynamics and Modelling of Ocean Waves, Cambridge, UK: Cambridge University Press, 1994.
- [10] MetOceanWorks, “Metocean Data Overview - Outer Dowsing Offshore Wind Farm,” MetOceanWorks, 2022.
- [11] K. Terzaghi, R. B. Peck and G. Mesri, Soil Mechanics in Engineering Practice, 3rd Ed, Wiley-Interscience, 1996.
- [12] K. Hasselmann, T. Barnett, E. Bouws, H. Carlson, D. Cartwright, K. Enke, J. Ewing, H. Gienapp, D. Hasselmann, P. Kruseman, A. Meerburg, P. Müller, D. Olbers, K. Richter, W. Sell and H. Walden, “Measurements of wind-wave growth and swell decay during the Joint North Sea Wave Project (JONSWAP),” *Ergänzungsheft zur Deutschen Hydrographischen Zeitschrift, Reihe A.*, 1973.
- [13] J. Battjes and H. Janssen, “Energy loss and set-up due to breaking random waves,” *Proceedings of the 16th International Conference on Coastal Engineering*, 2978.
- [14] Datawell BV, “A comparative report on the DWR MkIII and DWR4 data,” 2012.